Solvent-dependent excited state intramolecular proton transfer (ESIPT) pathways from phenol to carbon in 2,5-dihydroxyphenyl arenes

ARTICLE *in* PHOTOCHEMICAL AND PHOTOBIOLOGICAL SCIENCES · MAY 2013

Impact Factor: 2.27 · DOI: 10.1039/c3pp50091h · Source: PubMed

2 AUTHORS, INCLUDING:

Lily Wang
University of Victoria
11 PUBLICATIONS **57** CITATIONS

SEE PROFILE

Photochemical & Photobiological Sciences

RSC Publishing

PAPER

Solvent-dependent excited state intramolecular proton transfer (ESIPT) pathways from phenol to carbon in 2,5-dihydroxyphenyl arenes†

Cite this: *Photochem. Photobiol. Sci.*, 2013, **12**, 1571

Yu-Hsuan Wang and Peter Wan*

The ESIPT of three 2,5-dihydroxyphenyl-substituted arenes **9–11** was studied in various solvent systems, to investigate the direction of the proton transfer from the phenol to the respective carbons of naphthyl, phenanthrenyl and anthryl aromatic rings. In neat CH_3CN, **9–11** undergo direct ESIPT from the phenolic OH to the *ipso*-position of the corresponding aromatic carbon acceptors, *via* an intramolecular charge transfer state ($S_{1,ct}$), giving rise to observable zwitterions, ZIs **35**, **25**, **27**, respectively. Surprisingly, the generated ZI in **9** proceeds *via* a 1,2-phenyl migration followed by re-aromatization to afford **16** (a structural isomer of **9**) in quantitative yield. In **10** and **11**, the corresponding ZIs proceed *via* electrocyclic ring closure to furnish **20** and **28**, respectively. In the case of **10**, another intrinsic ESIPT pathway takes place to the 10-position of a phenanthrenyl ring, giving QM **26** in high quantum efficiency (Φ_{ex} = 0.72). In aqueous solution, **9** undergoes formal ESIPT to the more distal 2′- and 7′-positions of the naphthalene ring, delivering QMs **18** and **38**, which either revert back to the starting material or proceed *via* electrocyclic ring closure, respectively. In **11** in aqueous solution, formal ESIPT to the 10-position of the anthracene ring takes place delivering QM **29**, which readily aromatizes to regenerate starting material.

Received 18th March 2013,
Accepted 15th April 2013

DOI: 10.1039/c3pp50091h

www.rsc.org/pps

Introduction

Excited state intramolecular proton transfer (ESIPT) has been the subject of intensive investigations[1] since the pioneering work was reported by Weller.[2] This area is still of growing interest, mainly due to its fundamental nature as well as wide applications in systems such as photostabilizers,[3] fluorescent chemosensors,[4] scintillators,[5] solar collectors,[6] and laser dyes.[7] In general, an ESIPT mechanism involves a proton transfer from the donor (acidic site) to the acceptor (basic site) moiety caused by a simultaneous enhancement of both acidity and basicity in an electronic excited state. The best known ESIPT donor is the phenolic OH, which is much more acidic in the singlet excited state ($pK_a^* < pK_a$),[8] whereas the basic group is usually a heteroatom, such as a carbonyl oxygen or a heterocyclic nitrogen atom. Depending on the distance between the proton donor and the acceptor in the molecule, the ESIPT process can be further classified into direct ESIPT and formal (solvent-mediated) ESIPT.[9]

ESIPT to carbon atoms under neutral conditions usually takes place with very low quantum efficiency.[10] However, developing new carbon photoacids or photobases to initiate new chemistry is still of particular interest to us not only due to their potential industrial applications[11] but also for gaining new insights into mechanistic details of excited state acid–base chemistry.[12] Our group has discovered and documented new ESIPT systems where the proton transfer is from the phenolic OH to carbon atoms of adjacent aromatic moieties including phenyl,[13] naphthyl,[14,17] binaphthyl,[15] and anthryl[16] rings. These ESIPT reactions all require a reactive twisted conformation of the biaryl compound in the ground state, which allows for the overlap between the s-orbital of phenol OH and the adjacent aromatic π-system. In these systems, the enhanced acidity of phenolic proton in S_1 is sufficient to facilitate the intramolecular proton transfer.

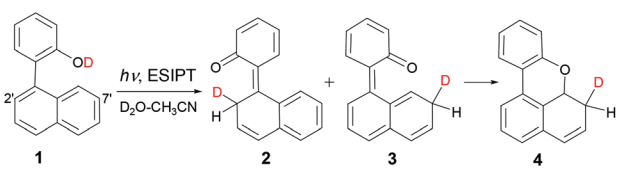

(1)

Department of Chemistry, University of Victoria, Box 3065, Victoria, British Columbia V8W 3V6, Canada. E-mail: pwan@uvic.ca; Fax: +1 (250)721-7147; Tel: +1 (250)721-8976

†Electronic supplementary information (ESI) available: Copies of the ^1H, ^{13}C NMR and 2D-spectra of all prepared and isolated compounds, UV-vis and fluorescence spectra of compounds **9–11**, fluoresence decay profile, transient absorption spectra obtained by LFP and computational data. See DOI: 10.1039/c3pp50091h

For example, ESIPT from the phenolic OH to the 2′- and 7′-naphthyl carbon atoms in 1-(2-hydroxylphenyl)naphthalene (**1**-OD) led to formation of two quinone methides (QMs) **2** and **3** with quantum yields of 0.14 (Φ_{ex}) and 0.2 (Φ_{cyc} for formation of **4**), respectively (eqn (1)). QM **2** undergoes reverse proton transfer to regenerate the deuterated starting material **1**-2′D, while QM **3** undergoes an electrocyclic ring closure to give isolable dihydrobenzoxanthene **4**. It was observed that ESIPT in **1** to both 2′- and 7′-positions requires water mediation.[14] We have recently reported a very efficient ESIPT, from phenol to aromatic carbon in 2-phenyl-1-naphthol that has the highest quantum efficiency (Φ_{ex} = 0.7) to date, *via* a conical intersection.[17]

In other developments, we reported a solvent-dependent ESIPT reaction in 9-(2,5-dihydroxyphenyl)anthracene (**5**): in aprotic solvents, the direct ESIPT to the 9-position of the anthracene moiety takes place to generate zwitterion (ZI) **6**, which leads to cyclised product **8**; whereas in protic solvents, the anticipated formal ESIPT to the 10-position occurs, to afford QM **7**, which then regenerates the starting material **5** or **5**-10D.[18] This study showed that in the excited state only the 2,5-dihydroxyphenyl chromophore (neither 2,4- nor 2,6-dihydroxyphenyl) exhibits this unique intramolecular charge transfer (ICT) emissive state, facilitating the proton transfer to the 9-position of the anthracene ring in aprotic solvents. That is, by utilizing the appropriate solvent, we can direct where the proton is transferred in the ESIPT. Comparing the ESIPT process in **5** with the parent compound 9-(2-hydroxyphenyl) anthracene,[16a] for the latter, only a water-mediated relay mechanism takes place, and no ESIPT process was observed in aprotic solvents. Therefore, special attention is paid to the employment of the 2,5-dihydroxyphenyl group serving as the proton donor upon excitation, which facilitates the formation of a significant CT excited state, leading to different ESIPT processes.

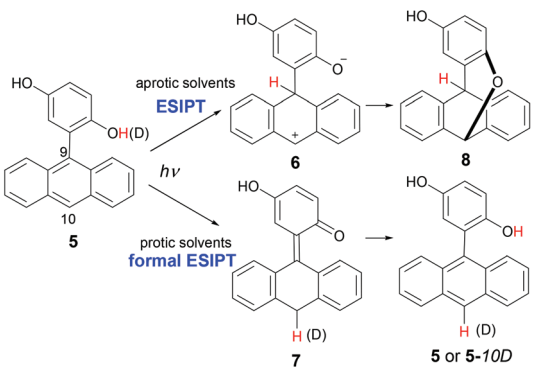

(2)

To explore whether the above ESIPT is applicable for other 2,5-dihydroxyphenyl arenes (DHPA), we considered derivatives for which naphthyl and phenanthrenyl groups are the proton accepting carbon bases. Thus, three new compounds **9–11** were synthesized to examine the influence of different accepting chromophores naphthyl, phenanthrenyl and anthryl rings on the efficiency and regioselectivity of ESIPT in both protic and aprotic solvents. That is, whether the solvent can play a key role to direct the proton transfer from phenolic OH of the 2,5-dihydroxyphenyl group to an adjacent aromatic carbon atom. Compound **9**, compared with the previously reported parent compound **1**, bears an additional hydroxyl group. As for **10**, a phenanthrene unit can be regarded as a benzonaphthalene moiety.[19] Furthermore, compound **11** with an extended phenyl ring at the 10-position, enhancing the conjugation, was chosen to investigate the potentially more stabilized ZI intermediate that could be best observed by laser flash photolysis (LFP). We show in this study that in addition to the anticipated formal ESIPT to 2′- and 7′-positions of an accepting naphthyl ring in the presence of water, a direct ESIPT in **9** to the *ipso*-position was observed in aprotic solvents, bringing about a rearrangement from a 1,2-phenyl ring shift, to give a photoisomerization product in relatively high yield. DHPAs **10** and **11** are also photochemically reactive in both aprotic and protic solvents, leading to different ESIPT processes. This is the first systematic study of ESIPT between ArOH and aromatic carbon in which the nature of the solvent directs the destination site of the proton transfer.

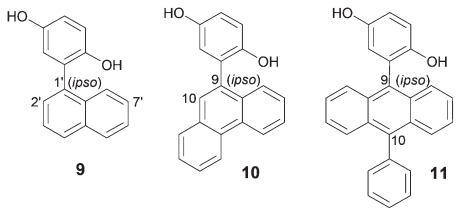

Results and discussion

Synthesis

The desired DHPA derivatives (**9–11**) were readily prepared by BBr_3 demethylation in high yields from the corresponding dimethoxy compounds **12**, **13**, and **15**, which were in turn synthesized according to slight modifications of the reported procedures[20] *via* Suzuki coupling reactions as shown in eqn (3) and (4). Additional details are provided in the ESI.† The synthetic route also provides the corresponding methyl ether compounds **12**, **13**, and **15**, which were directly compared with the photochemistry of the target DHPAs, to prove the necessity of the phenolic OH group in the observed ESIPT processes.

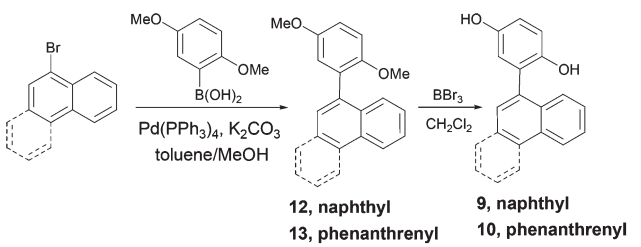

(3)

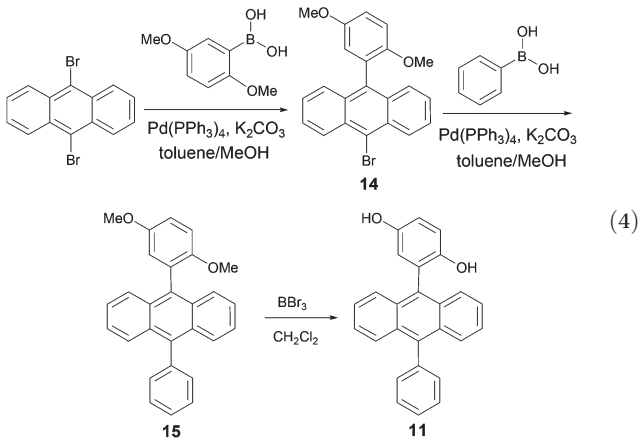

(4)

UV-vis spectroscopy

To probe photoreactivity and the ability to form stable photoproducts, **9–11** were initially examined by irradiations in argon-purged neat CH_3CN and H_2O–CH_3CN solvent systems in quartz cuvettes. After each exposure to 300 or 350 nm light (16 lamps), the UV-vis spectrum was taken (see ESI†). Photolyses of **9** in both neat CH_3CN and H_2O–CH_3CN (~10^{-5} M, λ_{ex} = 300 nm) led to dramatic changes in the absorption spectra with sharp isosbestic points, suggesting that **9** under both conditions reacts cleanly to give a different chromophore (Fig. 1). The characteristic absorption bands of **9** with maxima at 220 and 280 nm upon irradiation decreased in intensity with the concomitant growth of new absorption bands at 252, 300 and 371 nm in H_2O–CH_3CN, whereas a broadening of characteristic absorption bands in neat CH_3CN was detected. These two absorption spectra are clearly different, indicating that different photoproducts were formed in protic *vs.* aprotic solvents. It is worth noting that the photoproduct in Fig. 1(b) has finely structured new absorption bands with a significant red-shift relative to that of **9**, indicating that an enhanced conjugation between phenyl and naphthyl rings exists in the product.

Irradiation of **10** in neat CH_3CN (~10^{-5} M, λ_{ex} = 300 nm) led to drastic changes in the absorption spectra with well-defined isosbestic points at 272 and 320 nm and new absorption maximum at 375 nm, suggesting a clean transformation to give an enhanced rigid structure and conjugation. However, less efficient changes in the absorption spectra of **10** were observed on irradiation in H_2O–CH_3CN without a significant new band growing at longer wavelength. DHPA **11** possesses an intense anthracene absorption band at 260 nm and a weak but typical absorption band between 320 and 420 nm. Irradiation of **11** in neat CH_3CN or organic aprotic solvents such as diethyl ether, cyclohexane and THF (~10^{-5} M, λ_{ex} = 350 nm) gave rise to a rapid disappearance of the anthracene chromophore (Fig. 2), indicating the loss of the anthracene ring. The presence of sharp isosbestic points at 221, 305 and 313 nm suggests that a clean transformation is likely being formed without occurrence of secondary reactions. Presumably, in all of these solvent systems listed above, **11** undergoes the same photoreaction to give the same product, which is evidenced by later product

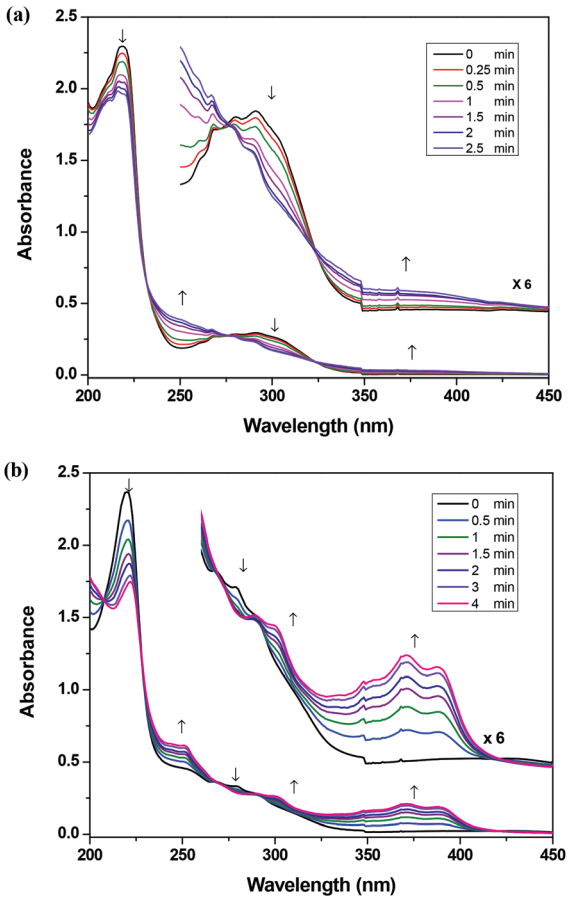

Fig. 1 UV-vis spectra showing the conversion of **9** in (a) neat CH_3CN, (b) 1 : 1 H_2O–CH_3CN (both argon saturated) with irradiation. Photolysis was carried out in a Rayonet photoreactor at 300 nm (16 lamps). Representative traces are shown with the corresponding irradiation times as given in the figure. The long wavelength region above 250 nm was expanded by 6-fold.

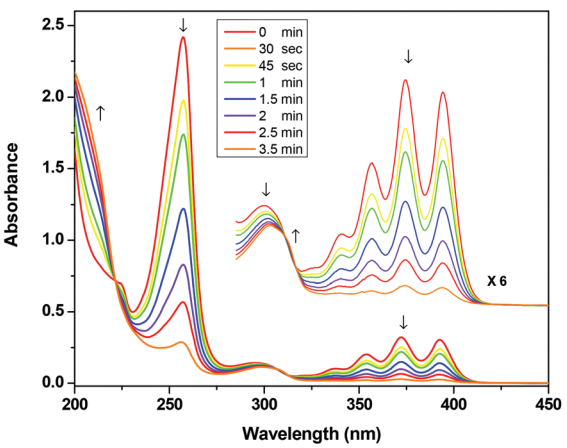

Fig. 2 UV-vis spectra showing the conversion of **11** in neat CH_3CN (argon saturated) with irradiation. Photolysis was carried out in a Rayonet photoreactor at 350 nm (16 lamps). Representative traces are shown with the corresponding irradiation times as given in the figure. The long wavelength region above 280 nm was expanded by 6-fold.

studies. In 1 : 1 H_2O–CH_3CN and 2,2,2-trifluoroethanol (TFE), the UV-vis spectra of **11** did not exhibit obvious changes of the anthracene absorption. We also examined another protic solvent, CH_3OH, and found a gradual decrease of anthracene chromophore absorbance with the recovery rate (several minutes) of absorbance at 370 nm after photolysis, indicating either more efficient photoreaction in CH_3OH than TFE and water or more long-lived photoproducts formed in CH_3OH that needs longer time to revert back to the starting material. These findings suggest that photolysis of **11** in protic solvents gives very short-lived photoadducts (trapped by water or CH_3OH), which quickly revert back to starting material (or that no photoproducts are formed). No notable absorption changes were observed on irradiation of the methyl ethers **12**, **13** and **15** in both neat and aqueous CH_3CN, consistent with the absorption changes coming from an ESIPT reaction for **9–11** that require the phenolic OH as the proton donor.

Product studies

In order to identify stable photoproducts, preparative scale irradiations were carried out for compounds **9–11** in various solvent systems (~10^{-3} M, deoxygenated, 300 or 350 nm, 16 lamps). The structure of each photoreaction product was determined by NMR characterization after isolation from the photolysate. Initial irradiation of **9** was performed in neat CH_3CN (1 h, 300 nm) giving rise to the primary photoisomerized photoproduct **16** in 37% conversion and a trace amount of benzofuran **17** (<3%) (eqn (5)). Prolonged irradiation of **9** for 10 h allowed quantitative formation of **16** along with the minor **17** isolated in 60% and 9% yields by preparative TLC on silica gel, respectively, without other observable side products. The structures of products **16** and **17** were determined and assigned by 1D and 2D NMR analyses (see ESI†). The same photoproducts were observed when irradiations were carried out in diethyl ether and cyclohexane, indicating that **9** proceeds *via* the same pathway in aprotic organic solvents. On the other hand, photolysis of **9** in H_2O–CH_3CN (1 : 9 (v/v)) under the same conditions gave a single isolable cyclization product **19** in 18% conversion. As reported previously (eqn (1)),[14] it is envisioned that **9** undergoes a water-mediated (formal) ESIPT from phenolic OH to the 7′-position to give QM **18**, followed by an electrocyclic ring closure to form dihydrobenzoxanthene **19** (eqn (6)).

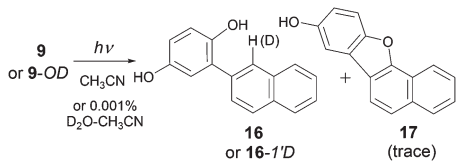

(5)

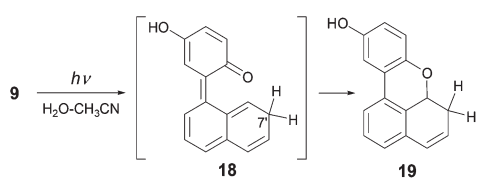

(6)

To monitor the ESIPT process involving the naphthalene as a carbon basic site for **9** in both aqueous and neat CH_3CN, we analyzed the deuterium incorporation into the recovered starting material and the photoproducts. Irradiations were typically carried out in both 0.001% and 10% D_2O–CH_3CN, followed by washing with H_2O after irradiations. Low concentration of D_2O is employed to supply only sufficient deuterium content to exchange the phenolic OH (to OD), and to avoid altering the reaction pathway. The extent and the position of deuteration were determined by NMR and MS. Photolysis of **9** (0.001% D_2O) for 1 h furnished 28% conversion of the starting material to give the corresponding deuterated photoisomerised product **16**-1′D. The disappearance of $H_{1'}$ at δ 7.98 of **16**-1′D in ^{1}H NMR is evidence that the phenolic OD was indeed transferred to the 1′-position. No indication of deuterium incorporation at other positions was observed. We can ascertain that the photoisomerised product **16** comes from a direct ESIPT to the 1′-position of the naphthalene ring, followed by a 1,2-phenyl shift and aromatization. In addition, irradiation of **9** (10% D_2O) under the same conditions yielded a mixture of **9**-2′D and **19**-7′D (eqn (7)), which were isolated on silica gel and analyzed by ^{1}H NMR. The recovered starting material (**9**-2′D) showed deuterium incorporation at the 2′-position (58%) of the naphthalene ring, while the cyclised product **19**-7′D (yield ~ 52%) showed exactly 50% of deuterium exchange of methylene hydrogens at the 7′-position similar to the mechanism proposed previously.[14] This finding indicates that one of the methylene hydrogens comes from either water (D_2O) or the phenolic OD, consistent with an intrinsic or water-mediated ESIPT from the phenol to the 7′-position responsible for the formation of **19**. The quantum yields of photogeneration of **9**-2′D and **19**-7′D in 10% D_2O–CH_3CN were determined by comparison with the deuterium incorporation of **1** as a secondary actinometer (Φ_{ex} = 0.14; Φ_{cyc} = 0.20)[14] to be 0.09 ± 0.01 and 0.012 ± 0.01, respectively. Also, the quantum yield for formation of **16** in neat CH_3CN was measured to be 0.06 ± 0.01 (Table 1).

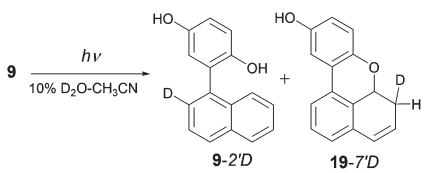

(7)

It is worth noting that the water concentration plays an important role in determining the ESIPT pathways of **9**, leading to either direct ESIPT or formal ESIPT processes. Three competing photochemical pathways found in **9** were determined by water content. Thus, to investigate the effect of water content on these proposed processes of **9**, solutions containing varying amounts of D_2O in CH_3CN were irradiated (Fig. 3). At very low water concentration (0–0.1 M D_2O), the formation of photoisomerized product **16** takes place without indication of deuterated **9**-2′D, showing that the reaction pathway is dominated by direct ESIPT to the 1′-position to give **16**-1′D. Increasing the D_2O content beyond the nominal

Table 1 Quantum yields for deuterium incorporation[a] and cyclization[b]

Compound	Φ_{ex}	Φ_{cyc}
1	0.14 ± 0.02[c]	0.20 ± 0.02[c]
5	0.03 ± 0.01[d]	0.12 ± 0.03
9	0.012 ± 0.01	0.09 ± 0.01
		0.06 ± 0.01[e]
10	0.72 ± 0.1	—[f]
		0.18 ± 0.03[g]
11	—[h]	0.13 ± 0.03
		0.78[i]

[a] Quantum yields of deuterium incorporation photolysed in 10% D_2O–CH_3CN at 300 nm for **9** and **10** whereas at 350 nm for **5** and **11**. The secondary actinometer employed for **9** and **10** was **1** (Φ_{ex} = 0.14);[14] for **11** was 9-(2-hydrophenyl)anthracene (Φ_{ex} = 0.09).[16a] [b] Quantum yields of cyclization photolysed in 10% D_2O–CH_3CN at 300 nm for **9** and in neat CH_3CN at 350 nm for **5** and **11**. [c] From ref. 14. [d] From ref. 18. [e] Quantum yield (Φ_{MeCN}) for the photogeneration of **16** in neat CH_3CN. [f] Quantum yield of cyclization in neat CH_3CN was too low to be measured. [g] Quantum yield (Φ_{MeOH}) for the photochemical formation of **24** in neat CH_3OH. [h] No observable deuterium exchange was detected. [i] Photolysed in diethyl ether.

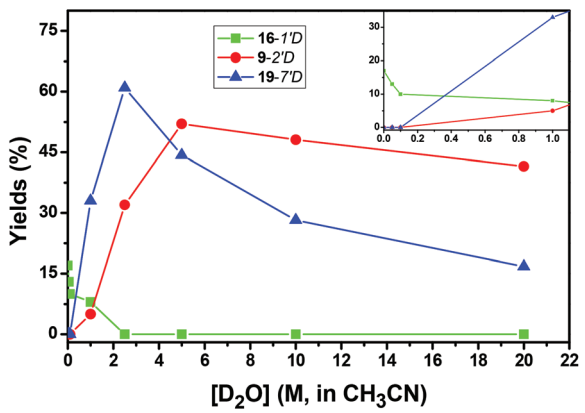

Fig. 3 Dependence of yields of **9**-2′D, photoisomerized product **16**-1′D, and photocyclization product **19**-7′D present in photolysate following photolysis of **9** in varying D_2O concentration in CH_3CN (~10^{-3} M, 300 nm, 16 lamps, 5 min). Yields in these runs were determined by ^{1}H NMR.

amount required for the exchange of the phenolic OH from **9** to **9**-OD led to a decrease in forming cyclization product **16**-1′D. No measurable deuteration incorporation at the 2′-position of **9** and cyclised product **19** was observed until about 1 M D_2O was reached, with **16**-1′D (8%), **9**-2′D (5%) and **19**-7′D (33%) co-existing. Presumably, this occurs when **9** was fully deuterated (to 9-OD) and the remaining D_2O mediated the ESIPT to 2′- and 7′-positions, to give **9**-2′D and **19**-7′D, respectively, with concomitant loss of proton transfer to form **16**-1′D. As more D_2O is added, the efficiency of formation of both **9**-2′D and **19**-7′D rose and reached a maximum at ~5 M and ~2.5 M, respectively, confirming that these photoproducts do not arise *via* intrinsic ESIPT. Gradual decrease in yields of **9**-2′D and **19**-7′D at higher water concentration (beyond 5 M D_2O) may be rationalized by the operation of competing ESPT to water to yield the phenolate $\mathbf{9}^-$. These results suggest that formation of **16**-1′D is *via* a direct ESIPT while generation of **9**-2′D and **19**-7′D is *via* a water-mediated ESIPT mechanism, in keeping with our expectation.

Photolysis of **10** was carried out in neat CH_3CN (~10^{-3} M, 300 nm, 16 lamps, 0.5 h) furnishing **20** (8%), **21** (<2%) and a trace amount of phenanthrene (eqn (8)). Prolonged irradiation (2 h) led to a significant amount of decomposition as noted by a broader aromatic region in ^{1}H NMR spectra and increase of isolated phenanthrene, suggesting that **20** is unstable. Attempts to isolate pure **20** were unsuccessful due to similar polarity with other side photoproducts and fast decomposition on silica gel. However, the structure of **20** was supported by the ^{1}H NMR spectrum, where a clear set of AB quartet signals (two benzylic hydrogens) was observed at δ 5.90 and δ 4.64 (J = 8.8 Hz) along with three hydrogens at the connecting phenol ring at δ 6.48 (dd, H_b), 6.60 (d, H_c), 6.65 (d, H_a). This finding suggests that **20** is formed *via* ESIPT from phenolic OH to the *ipso*-position of a phenanthrene ring, to give ZI **25**, followed by an intramolecular ring closure delivering **20**.

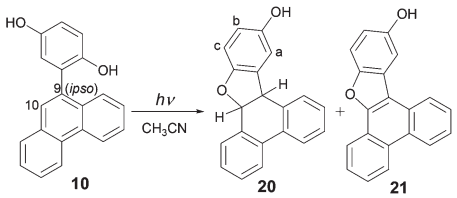

(8)

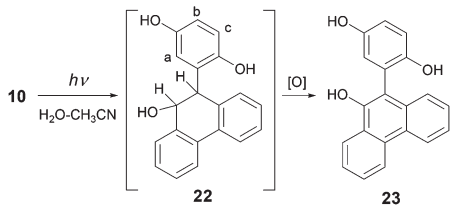

(9)

Irradiation of **10** (2 h) in 1 : 1 H_2O–CH_3CN gave rise to photoproduct **23** in 13% yield after chromatographic isolation from the photolysate (eqn (9)), whose structure was identified by NMR characterization. It is likely that **22** is the first formed photoproduct that could readily be oxidized to **23**, or revert back to starting material during the work-up or purification on silica gel. NMR analysis indicated that the crude reaction mixture was primarily a mixture of starting material and **22**, exhibiting a clear set of AB quartet signals at δ 5.07 and δ 4.63 (J = 7.0 Hz) with three hydrogens at the connecting phenol ring at δ 6.17 (d, H_a), 6.56 (dd, H_b), 6.69 (d, H_c), which are consistent with expectation for **22**. However, after chromatography, only **23** was isolated, supporting the assertion that **23** is formed from **22** during the work-up stage

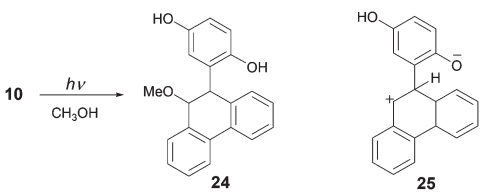

(10)

Photolysis of **10** was repeated (0.5 h), but the solvent changed to neat methanol. Methanol was chosen because it is a better nucleophile than water and better able to trap the anticipated QM or ZI intermediates,[21] which could possibly provide a chemically stable methyl ether photoadduct for NMR analyses. Indeed, a single photoproduct was isolated in relatively high yield (68%) and identified as methyl ether **24** by NMR analyses (eqn (10)). Extending the irradiation time to 3 h allowed quantitative formation of **24** (ratio of *trans*- and *cis*-isomer is 12 : 1 based on the integral of methoxy peaks at δ 3.34 and δ 3.35 from the crude ^{1}H NMR spectrum). The same photolysis of **10** was carried out in CD_3OD (0.5 h), where deuterium incorporation at the *ipso*-position of the phenanthrene ring was observed by the complete disappearance of the peak at δ 4.85. The photochemistry of **10** in aprotic and protic solvent systems appears to be similar, where a direct ESIPT from the phenolic OH to the *ipso*-position of the phenanthrene ring delivering ZI **25** occurs. This intermediate is then either attacked intramolecularly by phenolate to give **20** or intermolecularly by solvents (water or methanol) to give **22** and **24**, respectively.

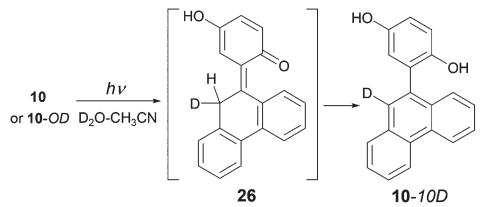

(11)

To probe other possible ESIPT processes available for **10**, we analyzed the deuterium exchange in the recovered starting material. Surprisingly, irradiation of **10** (300 nm, 8 lamps) in 10% D_2O–CH_3CN for 1 min efficiently led to deuterium incorporation at the 10-position (**10**-10D) (34%) of the phenanthrene ring. Also, irradiation of **10** at very low D_2O concentration (0.05 M) also gave rise to **10**-10D in quantitative yield, indicating that ESIPT is intrinsic. Presumably, direct ESIPT from phenolic OH to the 10-position would give the deuterated QM intermediate **26** which then undergoes reverse proton transfer to give deuterated starting material **10**-10D (eqn (11)). The quantum yield of **10**-10D was determined by comparison with the deuterium incorporation of **1** (Φ_{ex} = 0.14)[14] and 2-phenyl-1-naphthol (**31**) (Φ_{ex} = 0.7)[17] as secondary actinometers to give the quantum yield of 0.72 ± 0.1 (Table 1). Both actinometers gave similar results for the quantum yields of deuterium incorporation, with the mean value within the error of the measurements. To the best of our knowledge, this efficient ESIPT to carbon is the only one that is comparable with the ESIPT of 2-phenyl-1-naphthol (Φ_{ex} = 0.7) to date. Irradiation of **10** in 1 : 1 D_2O–CH_3CN (2 h) was also examined, furnishing a mixture of deuterated **10**-10D and **22**-9D10D. The complete disappearance of peaks at δ 5.07 and δ 4.63 in the crude ^{1}H NMR spectrum in **22** supports the assertion that ESIPT from phenolic OH to both 9- and 10-positions upon irradiation at higher water content. This finding could also imply that a direct ESIPT to the 10-position happened first and much more efficiently than ESIPT to the *ipso*-position of the phenanthrene ring, causing such low quantum efficiency for generating **20** and **22**.

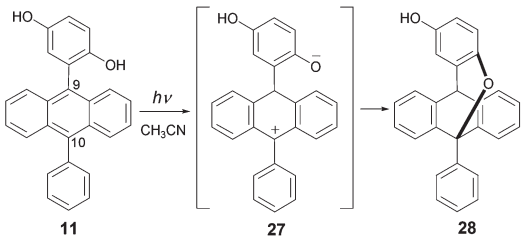

(12)

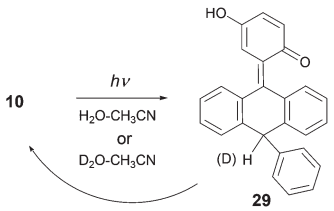

(13)

Irradiation of **11** (~10^{-3} M, 350 nm, 16 lamps, 5 min) in neat CH_3CN led to cyclised product **28** in 46% conversion (eqn (12)). It is envisioned that **11** undergoes direct ESIPT to the 9-position generating ZI **27**, followed by ring closure to give cyclised product **28**. As previously reported by our group,[18] photolysis of **5** in diethyl ether resulted in the higher quantum efficiency. Indeed, various aprotic solvents were tested and diethyl ether gave the highest quantum efficiency (Φ_{cyc} = 0.78). Photolysis of **11** in 1 : 1 H_2O–CH_3CN did not give rise to any isolable photoproducts; the starting material was recovered even under the long irradiation times (18 h), which is consistent with the results of UV-vis trace studies. Similar photolyses carried out in methanol and 10% D_2O–CH_3CN also resulted in no isolable photoproduct with observable deuterium exchange in the recovered starting material (detectable by NMR). It is most likely that **11** undergoes ESIPT to the 10-position to give QM **29** (eqn (13)), which readily reverts back to starting material.

Fluorescence measurements

ESIPT reactions of phenol derivatives involve the singlet excited state,[13–18] which can be studied by using steady state and time-resolved fluorescence, to provide additional mechanistic information. In particular, the efficient quenching of fluorescence emission by addition of water would provide evidence that the water-mediated ESIPT proceed from S_1.[1g,22] All fluorescence spectra were recorded in neat CH_3CN, aq. CH_3CN, and other selected organic solvents. Quantum yields of fluorescence were determined by using secondary reference quinine bisulfate (Φ = 0.55)[23] in 1.0 N H_2SO_4. Fluorescence lifetimes of **9–11** were obtained by single photon counting. The results are compiled in Table 2 and more details are given in ESI.†

Table 2 Photophysical and photochemical parameters for **9–11** and **15**[a]

Compound	λ_{em} [b]/nm	Φ_{ex} [c]	Φ_f [d]	τ_f [e] (ns)
9	308	414	0.069 ± 0.003	2.7 (55%), 1.2 (25%, 19 (20%)
10	298	415	0.021 ± 0.001	0.72 (92%), 3.3 (8%)
11	257, 297, 354, 373, 393	410, 425, 500 (sh)	0.008 ± 0.001	1.3 (93%), 8.5 (7%)
15	294 (sh), 335 (sh), 350, 368, 389	406, 425	0.079 ± 0.008	2.2 (92%), 1.6 (8%)

[a] Measurements were performed in neat CH_3CN. [b] Maxima in the absorption spectra. [c] Maxima in the emission spectra. [d] Fluorescence quantum yield measured by using quinine bisulfate (Φ_f = 0.55) in 1.0 N H_2SO_4.[23] [e] Fluorescence lifetimes in neat CH_3CN measured by time correlated single photon counting (SPC). Estimated error is ±0.1 ns.

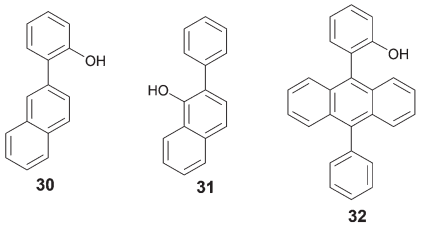

Based on the previous study of DHPA **5** (Φ_f = 0.003),[18] we assume that 2,5-dihydroxylphenyl derivatives may exhibit very weak fluorescence due to formation of an intramolecular charge transfer (ICT) state, leading to an efficient operation of ESIPT in aprotic solvents upon irradiation. Indeed, excitations of **9** and **10** in neat CH_3CN led to relatively weak fluorescence emissions with maxima at 414, 415 nm, respectively (Fig. 4). The observed Stokes shifts of **9** and **10** are quite large, indicating that there is a significant twisting about the biaryl bond toward planarity upon excitation to S_1. The high degree of twisting would allow for strong charge transfer from the hydroxyphenyl group to the naphthyl or phenanthrenyl ring in the excited state. Switching carbon bases or acceptors between naphthyl and phenanthrenyl rings does little to influence their emissive states. The fluorescence quantum yield for **10** in CH_3CN is 3 times lower than **9**, which could be rationalized by the operation of more efficient ESIPT in aprotic solvents for **10**. Compared to the structurally similar naphthyl derivatives **30** (Φ_f = 0.04)[24] and **31** (Φ_f = 0.03),[17] **10** exhibits essentially the same fluorescence quantum efficiency. This finding is consistent with the assertion that the intrinsic ESIPT deactivation pathway is operative from S_1 to give QM **26** or ZI **25**.

Unlike the typically strong and structured anthracene emission observed for most anthracenes, excitation of **11** in neat CH_3CN led to dual emission consisting of a fine-resolved emission at 425 nm and a structureless broad shoulder band at longer wavelengths (450–650 nm), attributed to the local excited (LE) and ICT states, respectively (Fig. 6). In contrast to **9** and **10**, fluorescence of **11** showed a relatively small Stokes shift, indicating small perturbation of the geometry for the fluorescent states. The introduction of a phenyl ring at the 10-position of the anthracene moiety compared to the parent compound **5** (Φ_f = 0.003)[18] resulted in a slight increase of fluorescence quantum yield to 0.008. Moreover, compared to previously reported anthracene derivative **32** (Φ_f = 0.93, τ_f = 8.7 ns),[16b] the introduction of extra phenolic OH at the *para*-position of the phenol ring in **11** (Φ_f = 0.008) leads to ~100 fold reduction in fluorescence quantum efficiency. These observations are consistent with a different photochemical pathway for **11** *vs.* **32** in neat CH_3CN (*viz.*, facile photocyclization for **32**).

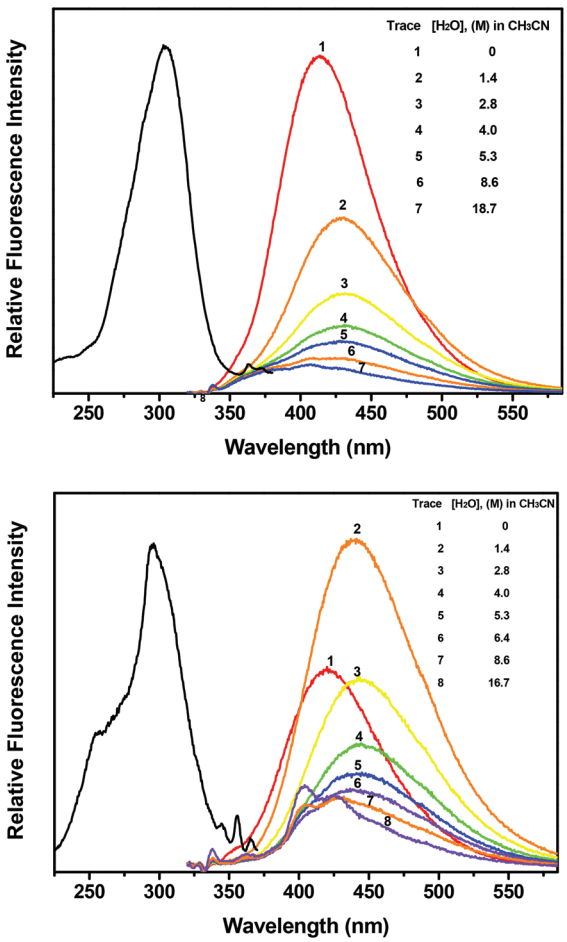

Fig. 4 Representative traces of **9** (top) and **10** (bottom) showing quenching of the fluorescence emission in neat CH_3CN by addition of water. Excitation wavelength λ_{ex} = 330 nm. Concentrations are shown in the figure.

Addition of small amounts of water (~1 M) to the CH_3CN solution of **9** resulted in an initial bathochromic shift of the emission to 429 nm, along with a dramatic quenching of the fluorescence intensity (Fig. 4). The decrease in fluorescence intensity with added water is consistent with an increase in

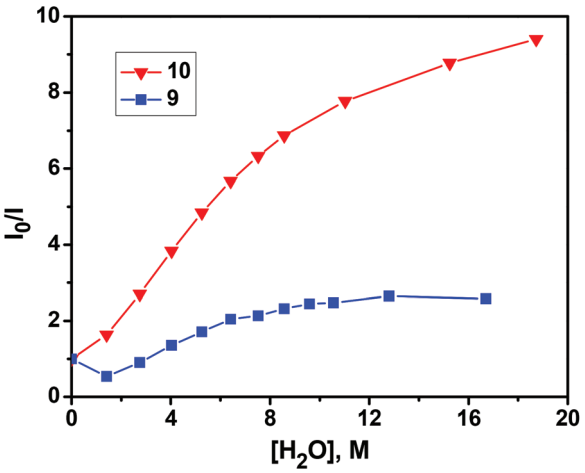

Fig. 5 Stern–Volmer plots of fluorescence quenching *vs.* water concentration in neat CH_3CN for **9** and **10**.

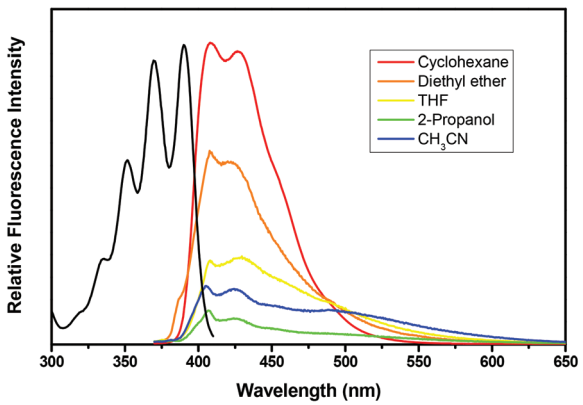

Fig. 6 Fluorescence emission spectra of **11** in various solvents (10^{-5} M). Excitation wavelength λ_{ex} = 360 nm. Emission wavelength λ_{em} = 420 nm.

product formation. On addition of a small amount of water (~1 M) to the CH_3CN solution of **10**, the fluorescence intensity increases two fold along with an initial bathochromic shift of the emission to 440 nm. It is assumed that water blocks the non-radiative deactivation pathway of ESIPT to the 10-position of the phenanthrene ring. Similar to the results found for **30** and **31**,[17,24] this behaviour can be rationalized by a very efficient intrinsic ESIPT pathway affording QM **26** that is partly quenched by addition of protic solvents. Addition of more water (>2.8 M) to **10** quenches the fluorescence as well as shifting the emission spectra hypsochromically at high water concentration (~12 M). Both results suggest that water quenching mainly comes from water-mediated ESIPT to form the corresponding QMs rather than the transfer of proton to the water (ESPT) to produce the excited state phenolates.

Stern–Volmer plots of the fluorescence quenching *vs.* water concentration in CH_3CN for **9** and **10** (Fig. 5) show typical non-linear behavior as previously observed in other direct and water-mediated ESIPT processes.[17] Compound **11** is not shown in this plot due to its weak emission in CH_3CN being unreliable for quenching studies. In **9**, at low water content (<7.5 M), quenching can be regarded as a polynomial function, which is consistent with an ESIPT where water clusters are involved in the deactivation of the singlet state, as reported in similar water-mediated ESIPT systems.[18,21,25] This finding could imply that fluorescence quenching within water content lower than 7.5 M results from the increasing efficiency of the formal ESIPT reaction to generate QMs. At a higher water concentration (>10 M), the quenching efficiency levels off. For **10**, with a small amount of water (<1.5 M), unlike the results found in **9**, a drop of fluorescence quenching with water concentration was shown, suggesting that the direct ESIPT is operative. At water concentrations above 1.5 M, the quenching increases linearly with the water concentration until 7 M, where the quenching efficiency levels off.

Fluorescence measurements of **11** in various solvents were also examined to obtain more insights into the properties of the singlet excited state. In a non-polar solvent, such as cyclohexane, **11** gives a single and fine-structured band with a maximum at 407 nm (Φ_f = 0.25), assigned to be the LE state (Fig. 6). With increasing solvent polarity, a dramatic decrease in the emission intensity accompanied with the growth of a new broad band at 500 nm was observed for **11**, indicating that the relative contributions of the LE (S_1) to the ICT ($S_{1,ct}$) states are controlled by solvent polarity. This observation is in agreement with the previous report for **5**,[18] where the dual fluorescence is rationalized by the proximity of $S_{1,ct}$ and S_1 states, giving rise to two emissive states (π,π^* and ICT). The finding is also in accord with higher efficiency of photocyclization upon photolyses of **11** in non-polar solvents given the proton transfer quenching of the ICT state. Based on the results from fluorescence and product studies, **11** most likely reacts (giving cyclization products) *via* the ICT state ($S_{1,ct}$).

Fluorescence lifetime for **9** was obtained by the three-exponential decay function, suggesting three emissive states (Table 2). The measured decays in neat CH_3CN are 2.7 (55%), 1.2 (25%) and 19 ns (20%) at a shorter wavelength of 400 nm, whereas 2.2 ns (92%) and 15 ns (8%) at a longer wavelength of 470 nm, implying that the shortest lifetime (1.2 ns) could be attributed to the ICT state. Fluorescence decay lifetimes of **10** and **11** were obtained by the two-exponential decay function, probably attributed to the presence of two excited singlet states, LE and ICT. In the case of **11**, two decays in neat CH_3CN were measured to be 1.3 (93%) and 8.5 ns (7%), assigned to ICT and LE states, respectively. Similar to the parent compound **5** with reported decay lifetimes to be 1.6 ns (ICT) and 3.4 ns (LE), the extended conjugation onto an anthracene chromophore in **11** does little to influence the lifetime of the ICT state.

Laser flash photolysis (LFP)

Although studying photoreactions by UV-vis spectroscopy can indicate intermediacy of long-lived transient species (>seconds), detecting short-lived zwitterions or carbocations requires nanosecond LFP. Thus, in order to characterize the proposed ZI and QM intermediates in the photochemistry of

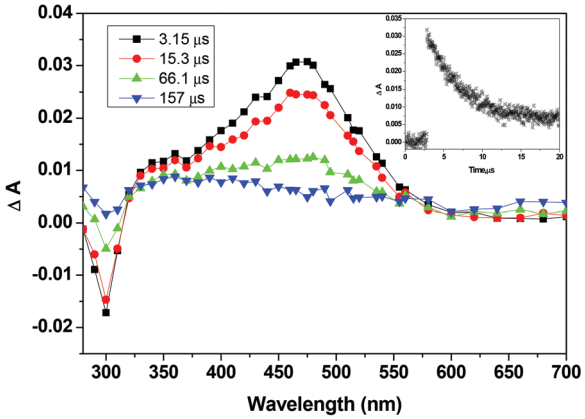

Fig. 7 Transient absorption spectra observed for **10** in O_2-purged CH_3CN solution. (Inset: decay at 480 nm.)

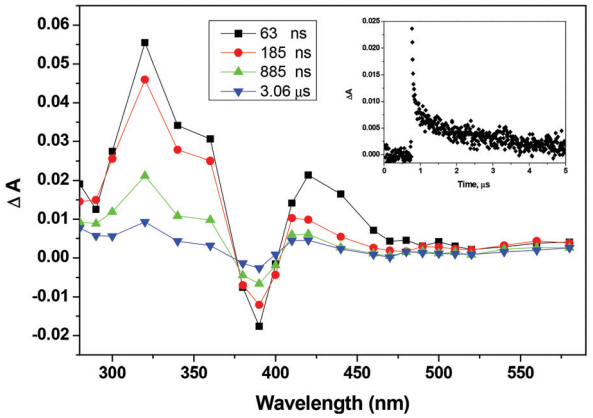

Fig. 8 Transient absorption spectra observed for **11** in O_2-purged CH_3CN solution. (Inset: decay at 420 nm.)

9–11, LFP was performed in neat CH_3CN and H_2O–CH_3CN (see ESI†). Our group has been able to successfully characterize a large variety of ZI and QM intermediates by LFP from ESIPT and other reactions.[26] LFP of **9** in N_2-purged solution CH_3CN gave rise to a strong transient absorption between 320 and 580 nm with a maximum at 460 nm. This transient decayed with $k = 6.7 \times 10^5$ s^{-1} (τ = 1.5 μs), and was strongly quenched by O_2 with $k = 1.6 \times 10^7$ s^{-1} (τ = 61 ns). Based on the similarity with spectra detected for other naphthylphenols,[24,27] and quenching by O_2, we assigned this transient to the phenol triplet–triplet absorption. The proposed ZIs **35** or **37** were not observed due to its anticipated weak signal and short lifetime.

LFP of **10** in CH_3CN under N_2 gave rise to a strong transient absorption in region of 380–550 nm with a maximum at 480 nm (Fig. 7). The transient absorption band at 480 nm decayed by second-order kinetics, giving lifetimes of 2.2 and 53 μs: the former was quenched by O_2 (τ = 51 ns), assignable to the triplet state; whereas the latter was not affected by O_2, probably corresponding to the QM **26**. Compared to the published spectra of similar structures,[27] we tentatively assigned this long-lived species (τ = 53 μs) to QM **26**. To verify if the observed longer-lived transient corresponds to QM **26**, LFP of its methoxy derivative **13** that cannot generate QM was also examined. In the transient spectra of **13** taken in CH_3CN under N_2, a signal that corresponds to the triplet was detected absorbing between 380 and 440 nm with a maximum at 420 nm, decaying in 1.6 μs (under O_2, τ = 40 ns). No other detectable longer-lived species was found at 480 nm, further providing a firm assignment of the long-lived transient to QM **26** observed by LFP of **10**.

Attempts to detect the ZI **33** for the parent compound **5** were unsuccessful perhaps due to its anticipated short lifetime (<20 ns). By introducing a phenyl ring at the 10-position of the anthracene ring, the anticipated ZI **27** can be stabilized by an extended conjugation system. Structurally similar to the anticipated ZI **27**, Basarić *et al.* recently reported the LFP of the photogenerated trityl ZI intermediate **34** giving rise to a transient at 420 nm with a lifetime of 7.5 μs.[27]

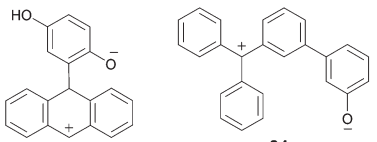

33 **34**

LFP of **11** in neat CH_3CN under N_2 led to a transient between 280 and 500 nm with a maximum at 420 nm, decaying in 61 μs, along with a bleaching signal at 390 nm (Fig. 8). This bleaching signal resulted from the absorption of the laser flash by the substrate. The recovery of the bleaching to the baseline after longer time scale delays indicates the good reversibility of the process initiated by the laser flash. Saturating the solution with oxygen quenched the lifetime to 63 ns. This transient is assigned to the triplet state of **11** based on similarity to known T–T absorption detected for other anthracene derivatives.[16] However, the transient at 420 nm decayed by second-order kinetics, giving lifetimes of 63 ns and 2.8 μs. For the corresponding methoxy derivative **15**, LFP in neat CH_3CN under O_2 yielded a similar transient at 420 nm, decaying in a single-exponential fashion ($\tau \sim$ 50 ns), assignable to the triplet state of **15**. Unlike the transient observed in **11**, no other detectable longer-lived species was detected in **15** at 420 nm except for triplets, providing further evidence that the other decay observed in **11** could be assignable to the trityl cation **27**. The anticipated ZI **27** has a trityl cation as a chromophore, and should absorb around 420 nm.[26,28,29] Therefore, we tentatively assign the long-lived species ($\tau \sim$ 2.8 μs) to ZI **27**, which has a similar decay lifetime to ZI **34**.

In both N_2 and O_2-purged H_2O–CH_3CN solutions, LFP of all **9**, **10** and **11** led to relatively weak transient absorptions, which precluded further study. The proposed intermediates QMs **18** and **38**, structurally similar to QMs **2** and **3**, should absorb at 360–560 nm,[14] where the T–T absorption was usually detected. As for QM **29**, in addition to the spectral interference from the triplet signals, substrate bleaching of the anthracene chromophore obscured its transient spectra. Hence, due to their short

lifetimes, overlapping with the triplets, as well as their very low quantum efficiency of formation their detection was not possible.

Photochemical reaction mechanisms

Based on the above data from product studies, deuterium exchange, fluorescence measurements, and LFP, the mechanism of photoreactions of **9–11** can now be proposed.

Excitation of **9** to S_1 in aprotic solvents such as CH_3CN or diethyl ether (or with low H_2O content) resulted in initial direct ESIPT delivering ZI **35**, as demonstrated by deuterium exchange observed at the 1′-position of photoisomerized product **16** (Scheme 1). ZI **35** proceeds *via* either rotation of the phenyl–naphthyl bond (blue arrow) to facilitate ring closure, to give possible cyclised product **36**, or *via* protonation to revert back to the starting material. However, **36** was not observed. A faster process apparently is a phenyl shift (red arrow) to form a more stable benzylic carbocation **37** instead. ZI **37** then rapidly undergoes proton transfer affording the major observed photoproduct **16**, which on further photolysis can lead to **17** as a minor product. **17** could also form directly from **37**. Although both 2,5-dihydroxyphenyl naphthyl derivatives (**9** and **16**) are well known compounds,[28,30] this kind of photo-initiated transformation of two regioisomers has not been reported before.

Excitation of **9** in the aqueous media leads to formal ESIPT (Scheme 2), as indicated by fluorescence quenching with added water and deuterium exchange at 2′- and 7′-positions of the naphthyl ring. As shown in Scheme 2, a water-mediated ESIPT in **9**-OD from phenol to the 2′- and 7′-carbon atoms on the naphthyl ring gives rise to the QM intermediates **38** and **18**, respectively. The former undergoes tautomerization to furnish deuterated starting material **9**-2′D, whereas the latter proceeds *via* electrocyclic ring closure to give cyclised **19**-7′D. Measured quantum yields for deuterium incorporation and cyclization indicate that ESIPT to the 7′-carbon is an order of magnitude more efficient than to the 2′-carbon. This mechanism is consistent with the previous report for the parent compound **1**.[14] Excitation of **10** in both aprotic and protic solvent systems resulted in direct ESIPT to both 9 (*ipso*)- and 10-

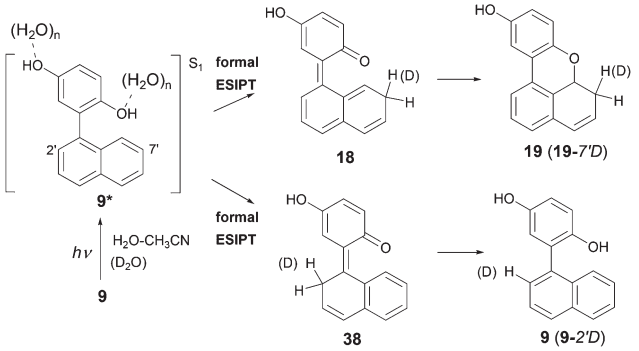

Scheme 2

positions of the phenanthrenyl ring giving rise to ZI **25** and QM **26**, respectively (Scheme 3). The fate of ZI **25** depends on the solvent system. In neat CH_3CN, ZI **25** undergoes a rotation (blue arrow) about the phenyl–phenanthrene ring bond to facilitate intramolecular ring closure giving rise to **20**. However, **20** is unstable and is readily oxidized to **21**. In CH_3OH and aqueous solution, ZI **25** undergoes nucleophilic quenching by CH_3OH or H_2O (red arrow), delivering **24** or **22**, respectively. Photoadduct **22** is unstable and can readily eliminate water to regenerate starting material or oxidized to give **23**. The quantum yields for photogeneration of **20** and **22** are relatively low. This is explained by a competing ultrafast intrinsic ESIPT pathway from phenolic OH to the 10-position, delivering QM **26** which upon tautomerization regenerates deuterated starting material **10**-10D (Φ_{ex} = 0.72) in the presence of D_2O. QM **26** could also be trapped by CH_3OH (or water) to give photoadduct **39**, however, it could also rapidly revert back to starting material so that we were unable to detect it. Evidence for QM **26** formation was supported by formation of **10**-10D and LFP studies of **10** (τ = 53 μs). In addition, deuterium incorporation was observed at both 9- and 10-positions in photoadducts **22** and **24** when photolyses were carried out in 1 : 1 D_2O–CH_3CN and CD_3OD, respectively. Since a relatively high efficiency of direct ESIPT to the 10-position over the *ipso*-position of the phenanthrene ring was observed in **10**, it is most likely the formation of QM **26** occurs first to regenerate

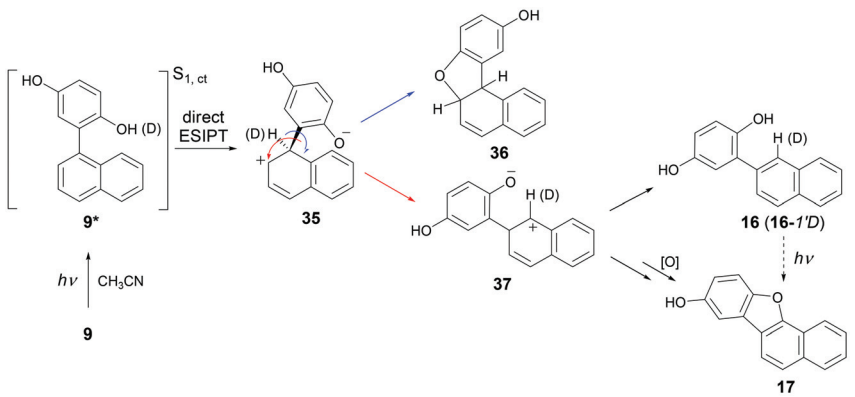

Scheme 1

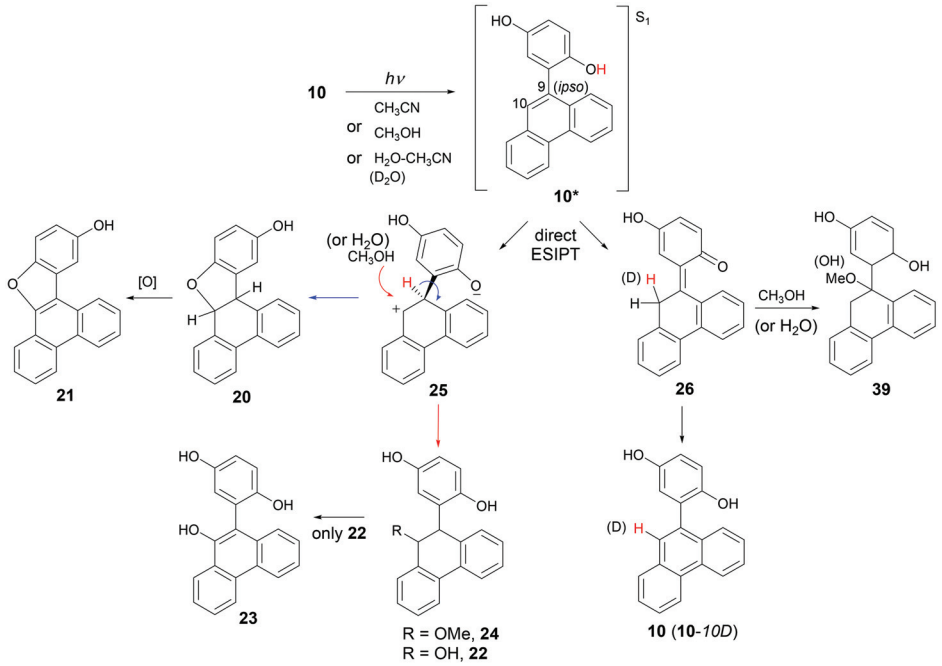

Scheme 3

10-10D, followed by the photoaddition by CH_3OH or water *via* ZI **25**. Consequently, we conclude that upon irradiation of **10** in either protic or aprotic solvents, there are two direct ESIPT pathways competing: the major one is to the 10-position of the phenanthrene ring delivering QM **26**; the minor is to the 9 (*ipso*)-position giving rise to ZI **25**.

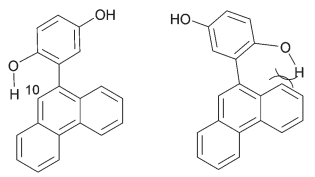

The reason for the observed high quantum efficiency (Φ_{ex} = 0.72) in **10** may be due to the possible conical intersections with the S_0 dominating the deactivation pathway from the singlet excited state surface as previously reported in studies of structurally similar naphthols **30** and **31**.[17,24] Furthermore, considering the possible *syn* or *anti* conformers of **10** in the ground state population equilibrium as discussed for naphthol derivative **31**,[24] it is assumed that one of the *syn* conformers (**S10-1**) dominates favouring the direct ESIPT to the 10-position whereas the other *syn* conformer (**S10-2**) is unfavorable due to being hindered by a connected phenyl ring of the phenanthrene moiety as shown. Based on B3LYP/6-311 calculations, **S10-1** is lower in energy than **S10-2**. That is, in **10**, the ground state conformational equilibrium effectively facilitates direct ESIPT to the 10-position of the phenanthrene ring, leading to a very high quantum efficiency of deuterium incorporation of **10**.

Similar to **5**, the reaction mechanism of **11** in aprotic solvents such as CH_3CN and diethyl ether is direct ESIPT from the phenol to the 9-position to generate ZI intermediate **27**, which upon bond rotation and ring closure gives cyclised product **28** (Scheme 4). As demonstrated in fluorescence

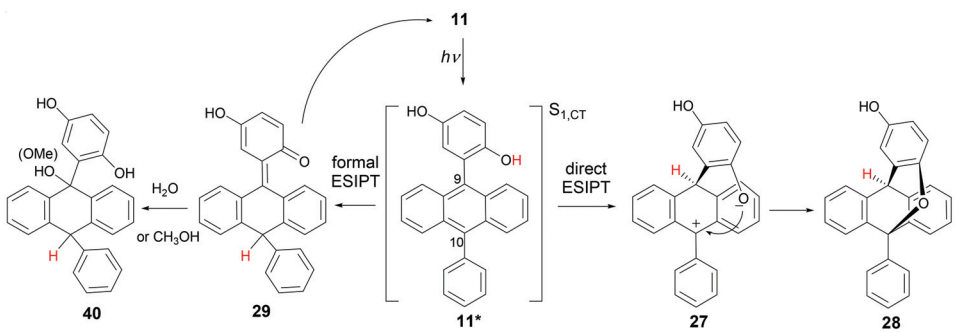

Scheme 4

studies, the ESIPT is *via* an ICT emissive state. Evidence for intermediate **27** was provided by LFP studies which showed formation of a triaryl methyl carbocation with a lifetime ~ 2.8 μs at λ_{max} = 420 nm, consistent with that reported in the literature.[28,29] Very high quantum efficiency of photocyclization was observed in diethyl ether (Φ_{cyc} = 0.78). A water-mediated ESIPT process could also be initiated upon irradiation of **11** in the presence of protic solvents, delivering QM **29**, which is in accord with the previous report of the related systems.[18] Nucleophilic attack of QM **29** could take place at the 9-position by water or methanol, but these products could not be isolated presumably due to their facile reversion back to starting material.

Conclusions

2,5-Dihydroxyphenyl derivatives **9–11** were synthesized and their photochemistry and photophysics investigated in various solvent systems. This work demonstrates that the solvent plays a key role in determining details of proton transfer from phenolic OH of the 2,5-dihydroxyphenyl ring to the anticipated positions of the carbon bases in **9–11**. In an aqueous solvent, upon excitation to the S_1, **9** and **11** undergo water-mediated ESIPT from phenolic OH to the specific carbons of the connecting aromatic ring, delivering QM intermediates, which could either revert back to the starting materials or proceed *via* cyclization. In aprotic solvents, **9–11** all undergo direct ESIPT from phenolic OH to the *ipso*-positions *via* intramolecular charge transfer states ($S_{1,ct}$), giving rise to the corresponding ZIs **35**, **25**, **27**, respectively. Interestingly, the generated ZI in **9** was followed by a 1,2-phenyl shift, furnishing the photoisomerization product **16** in quantitative yield. In **10** and **11**, the corresponding ZIs proceed *via* ring closure (collapse of the ZIs) to furnish **20** and **28**, respectively. Two or three competing photochemical pathways for **9–11**, formal ESIPT *vs.* direct ESIPT, are controlled by the selection of solvent and water concentration.

Experimental section

General

All NMR spectra were recorded on Bruker AC300 (300 MHz) and Avance 500 (500 MHz) instruments. For the structural assignment of signals, 2D homonuclear COSY and NOESY and heteronuclear HSQC and HMBC techniques were used. Melting points were determined using a Gallenkamp melting point apparatus (and were not corrected). UV-Vis spectra were taken on a Varian Cary 1 spectrophotometer at rt. IR spectra were recorded on a spectrophotometer in KBr. Accuracy mass analysis was carried out at the UVIC Genome BC Proteomics Centre. A mg mL^{-1} solution of the analyte was diluted by a factor of 10–100 and injected by liquid infusion at ~300–500 nL min^{-1} by a syringe pump through a nano-ESI source, and all solvents used were of MS grade. All the irradiation experiments were performed in a Rayonet photochemical reactor equipped with 16 lamps of 300 nm or 350 nm as indicated. During irradiations, solutions were purged with a stream of argon and cooled by a tap water cold finger condenser. Acetonitrile for photolysis was of HPLC grade. Other solvents (ACS grade) used for synthesis were purchased from Aldrich and used as received. Preparative TLC was carried out on silica gel GF Uniplates (20 cm × 20 cm) and purchased from Analtech. $CDCl_3$, D_2O and CD_3CN were purchased from Cambridge Isotope Laboratory.

Materials

1-Bromonaphthalene, 9-bromophenanthrene, 9,10-dibromoanthracene, 2,5-dimethoxyphenyl boronic acid, phenylboronic acid, $Pd(PPh_3)_4$, and BBr_3 (1.0 M solution in CH_2Cl_2) were purchased from Aldrich and used upon received. DHPA derivatives **9–11** were readily obtained from the corresponding dimethoxy derivatives **12**, **13** and **15** by employing BBr_3 demethylation reaction. **12**, **13** and **15** were then prepared from Suzuki coupling reactions according to the described procedures.[12b,17]

General procedure for Suzuki coupling reaction

A mixture of 1 equiv. of bromo compound and 1.1 equiv. (or 1.0 equiv. whereas indicated) of boronic acid was dissolved in a mixture of toluene (15 mL) and MeOH (5 mL) in a 100 mL round-bottom flask. To the reaction mixture was added 2 equiv. of K_2CO_3 and 3 mol% of tetrakis-triphenylphosphine palladium $Pd(PPh_3)_4$ and the mixture was heated at reflux for 24 h under an N_2 atmosphere. The reaction mixture was then cooled to room temperature and to the mixture was added H_2O (20 mL). The two layers were separated and the aqueous layer was extracted with CH_2Cl_2 (3 × 10 mL). The combined organic layers were washed with brine and dried over anhydrous $MgSO_4$. After filtration, concentration under reduced pressure afforded the crude product. Purification of the residue was achieved by flash column chromatography on silica gel using ethyl acetate in an *n*-hexane mixture (EtOAc–hexane gradient, 0% to 10%) as an eluent.

1-(2,5-Dimethoxyphenyl)naphthalene (12).[20a,30b] Following the general procedure, a mixture of 650 mg (3.14 mmol) of 1-bromonaphthalene and 629 mg (3.45 mmol) of 2,5-dimethoxyphenylboronic acid in the presence of K_2CO_3 (867 mg, 6.28 mmol) and $Pd(PPh_3)_4$ (109 mg, 0.09 mmol) was converted to 646 mg (78%) of the product **12** as a colorless crystal. Mp 91–92 °C (Lit.[30b] mp = 94 °C); ^{1}H NMR (500 MHz, $CDCl_3$) δ 7.87 (d, J = 8.5 Hz, 1 H), 7.85 (d, J = 8.3 Hz, 1 H), 7.60 (d, J = 8.6 Hz, 1 H), 7.51 (dd, J = 8.3, 8.0 Hz, 1 H), 7.45 (td, J = 7.6, 1.2 Hz, 1 H), 7.41–7.36 (m, 2 H), 6.97 (d, J = 8.8 Hz, 1 H), 6.94 (dd, J = 8.8, 2.8 Hz, 1 H), 6.86 (d, J = 2.8 Hz, 1 H), 3.78 (s, 3 H, OMe), 3.62 (s, 3 H, OMe); ^{13}C NMR (125 MHz, $CDCl_3$) δ 153.5, 151.5, 136.8, 133.4, 132.0, 130.5, 128.1, 127.7, 127.2, 126.4, 125.7, 125.6, 125.3, 117.6, 113.7, 112.4, 56.3, 55.8.

1-(2,5-Dimethoxyphenyl)phenanthrene (13).[20a] Following the general procedure, a mixture of 500 mg (1.94 mmol) of 9-bromophenanthrene and 389 mg (2.14 mmol) of 2,5-dimethoxyphenylboronic acid in the presence of K_2CO_3 (535 mg,

3.88 mmol) and $Pd(PPh_3)_4$ (67.3 mg, 0.06 mmol) was converted to 501 mg (82%) of the product **13** as a colorless crystal. Mp 150–152 °C; ^{1}H NMR (300 MHz, $CDCl_3$) δ 8.75 (d, J = 8.5 Hz, 1 H), 8.72 (d, J = 8.6 Hz, 1 H), 7.88 (dd, J = 7.8, 1.4 Hz, 1 H), 7.68 (s, 1 H), 7.67–7.57 (m, 5 H), 7.53–7.47 (m, 1 H), 6.99–6.97 (m, 2 H), 6.95–6.93 (m, 1 H), 3.81 (s, 3 H, OMe), 3.63 (s, 3 H, OMe); ^{13}C NMR (75 MHz, $CDCl_3$) δ 153.7, 151.8, 135.7, 131.7, 131.3, 130.6, 130.25, 130.2, 128.7, 127.7, 127.2, 126.6, 126.5, 126.34, 126.3, 122.7, 122.6, 117.6, 113.8, 112.4, 56.4, 55.8.

9-Bromo-10-(2,5-dimethoxyphenyl)anthracene (14). Following the general procedure, a mixture of 800 mg (2.38 mmol) of 9,10-dibromoanthracene and 433 mg (2.38 mmol) of 2,5-dimethoxyphenylboronic acid in the presence of K_2CO_3 (647 mg, 4.76 mmol) and $Pd(PPh_3)_4$ (82.5 mg, 0.07 mmol) was converted to 709 mg (76%) of the product **14** as a yellowish solid, mp 147–148 °C; ^{1}H NMR (500 MHz, $CDCl_3$) δ 8.59 (d, J = 8.8 Hz, 2 H), 7.64 (d, J = 8.6 Hz, 2 H), 7.57 (ddd, J = 8.8, 8.7, 1.1 Hz, 2 H), 7.37 (ddd, J = 8.8, 8.7, 1.1 Hz, 2 H), 7.06 (d, J = 1.8 Hz, 2 H), 6.83–6.82 (t, J = 1.8 Hz, 1 H), 3.78 (s, 3 H, OMe), 3.53 (s, 3 H, OMe); ^{13}C NMR (125 MHz, $CDCl_3$) δ 153.8, 152.4, 134.5, 131.2, 130.5, 128.1, 127.4, 127.1, 125.7 123.0, 118.3, 114.6, 112.9, 56.6, 56.0; IR ($CHCl_3$, cm^{-1}) 3853, 3744, 2934, 2831, 1497, 1423, 1224, 1046, 903, 760.

9-(2,5-Dimethoxyphenyl)-10-phenylanthracene (15). Following the general procedure, a mixture of 671 mg (1.71 mmol) of **14** and 230 mg (1.88 mmol) of phenylboronic acid in the presence of K_2CO_3 (472 mg, 3.42 mmol) and $Pd(PPh_3)_4$ (57.8 mg, 0.05 mmol) was converted to 627 mg (94%) of the product **15** as an off-white solid, mp 201–203 °C; ^{1}H NMR (300 MHz, $CDCl_3$) δ 7.71–7.67 (m, 4 H), 7.63–7.47 (m, 5 H), 7.37–7.30 (m, 4 H), 7.13 (d, J = 8.9 Hz, 1 H), 7.09 (dd, J = 8.9, 2.7 Hz, 1 H), 6.91 (d, J = 2.7 Hz, 1 H), 3.82 (s, 3 H, OMe), 3.61 (s, 3 H, OMe); ^{13}C NMR (75 MHz, $CDCl_3$) δ 153.8, 152.5, 139.2, 137.1, 133.6,131.5, 131.4, 130.0, 129.9, 128.7, 128.4, 127.4, 127.1, 126.9, 125.0, 124.96, 118.3, 114.3, 112.8, 56.6, 55.8; IR ($CHCl_3$, cm^{-1}) 3055, 2933, 2825, 1495, 1428, 1269, 1222, 1045, 766; MS (ESI) m/z 391 (M^+ + 1), 390 (M^+); HRMS, calcd for $C_{28}H_{22}O_2$: 391.16925 (M^+ + H); Found 391.17047.

General procedure for BBr_3 demethylation reaction

To a solution of the methoxy compound in CH_2Cl_2 (20 mL) at 0 °C was added 5 equiv. of BBr_3 (1 M in CH_2Cl_2) drop-wise under N_2. The ice bath was removed and the reaction mixture was stirred at room temperature for an additional 3 h under N_2. The reaction mixture was quenched by CH_3OH (10 mL) and stirred for 10 min. Followed by addition of water, the mixture was extracted with CH_2Cl_2 (3 × 10 mL) and the combined organic layers were dried over anhydrous $MgSO_4$. After filtration, the solvent was removed on a rotary evaporator. The crude residue was then purified by flash column chromatography on silica gel using 0–10% of CH_2Cl_2 in ethyl acetate as an eluent and further purified by crystallization from methylene chloride and *n*-hexanes.

1-(2,5-Dihydroxyphenyl)naphthalene (9).[30b] From 640 mg (2.42 mmol) of 1-(2,5-dimethoxyphenyl)naphthalene (**12**) and a solution of BBr_3, the reaction gave the crude product that was purified by flash column chromatography on silica gel (CH_2Cl_2–hexane gradient, 0% to 10%) to afford 526 mg (92%) of the product **9** as an off-white solid. Mp 108–110 °C (Lit.[30b] mp = 83–84 °C); ^{1}H NMR (500 MHz, $CDCl_3$) δ 7.91 (d, J = 8.4 Hz, 2 H, H-2, H-8), 7.67 (d, J = 8.7 Hz, 1 H, H-5), 7.55 (dd, J = 8.4, 8.35, 1 H, H-3), 7.51 (dd, J = 8.4 Hz, 8.1 Hz, 1 H, H-7), 7.47–7.44 (m, 2 H, H-4, H-5), 6.93 (d, J = 8.7 Hz, 1 H, H-11), 6.84 (dd, J = 8.7 Hz, 3.1 Hz, 1 H, H-12), 6.75 (d, J = 3.1 Hz, 1 H, H-14), 4.55 (s, 1 H, OH_a), 4.45 (s, 1 H, OH_b); ^{13}C NMR (125 MHz, $CDCl_3$) δ 149.0 (s, C-10), 147.1 (s, C-13), 133.9 (s, C-1), 133.7 (s, C-15), 131.6 (s, C-11), 128.9 (d, C-2/C-8), 128.4 (d, C-2/C-8), 128.0 (d, C-4), 127.0 (s, C-9), 126.8 (d, C-6), 126.4 (d, C-7), 125.7 (d, C-3), 125.5 (d, C-5), 117.5 (d, C-11), 116.4 (d, C-12/C-14), 116.3 (d, C-12/C-14); IR ($CHCl_3$, cm^{-1}) 3381, 3075, 3046, 2360, 1650, 1491, 1437, 1203, 735.

1-(2,5-Dihydroxyphenyl)phenanthrene (10). From 500 mg (1.59 mmol) of 1-(2,5-dimethoxyphenyl)phenanthrene (**13**) and a solution of BBr_3, the reaction gave the crude product which was purified by recrystallized from methylene chloride to afford 455 mg (96%) of the product **10** as an off-white crystal, mp 188–190 °C; ^{1}H NMR (500 MHz, CD_3CN) δ 8.82 (d, J = 8.3 Hz, 1 H, H-4/H-5), 8.79 (d, J = 8.4 Hz, 1 H, H-4/H-5), 7.95 (d, J = 8.1 Hz, 1 H, H-1), 7.72–7.63 (m, 4 H, H-3, H-6, H-2, H-7), 7.70 (s, 1 H, H-10) 7.56 (dd, J = 8.4, 8.0 Hz, 1 H, H-8), 6.84 (d, J = 8.8 Hz, 1 H, H-13), 6.80 (dd, J = 8.8, 2.8 Hz, 1 H, H-12), 6.74 (d, J = 2.8 Hz, 1 H, H-11), 6.03 (s, 1 H, OH), 4.65 (s, 1 H, OH); ^{13}C NMR (125 MHz, CD_3CN) δ 151.2, 148.7, 136.1, 132.8, 132.2, 131.4, 131.1, 129.7, 129.2, 128.8, 128.1, 127.94, 127.9, 127.8, 127.75, 124.0, 123.7, 118.7, 117.6, 116.9; IR ($CHCl_3$, cm^{-1}) 3701, 3675, 3566, 3470, 1655, 1455, 1203, 725; MS (ESI) m/z 285 (M^+ − H); HRMS, calcd for $C_{20}H_{14}O_2$: 285.09211 (M^+ − H); Found 285.09186.

9-(2,5-Dihydroxyphenyl)-10-phenylanthracene (11). From 654 mg (1.68 mmol) of 9-(2,5-dimethoxyphenyl)-10-phenylanthracene (**15**) and a solution of BBr_3, the reaction gave the crude product which was purified by flash column chromatography on silica gel (EtOAc–hexane gradient, 20% to 30%) and recrystallized from methylene chloride and hexanes to afford 516 mg (85%) of the product **11** as a colorless crystal, mp 220–221 °C; ^{1}H NMR (500 MHz, $CDCl_3$) δ 7.74 (d, J = 8.6 Hz, 2 H, H-1/H-4), 7.70 (d, J = 8.3 Hz, 2 H, H-1/H-4), 7.62–7.53 (m, 3 H, H-6 and H-7), 7.47–7.45 (m, 2 H, H-5), 7.41–7.33 (m, 4 H, H-2 and H-3), 7.06 (d, J = 8.8 Hz, 1 H, H-10), 6.97 (dd, J = 8.8, 3.2 Hz, 1 H, H-9), 6.80 (d, J = 3.2 Hz, 1 H, H-8), 4.65 (s, 1 H, OH), 4.29 (s, 1 H, OH); ^{13}C NMR (125 MHz, $CDCl_3$) δ 149.3, 148.0, 138.7, 138.6, 131.2, 131.1, 130.3, 130.1, 129.4, 128.5, 127.7, 127.3, 126.1, 126.05, 125.4, 125.1, 118.5, 116.8, 116.6; IR ($CHCl_3$, cm^{-1}) 3670, 3619, 3470, 3356, 1653, 1456, 1198, 913, 748; MS (ESI) m/z 361(M^+ − H); HRMS, calcd for $C_{20}H_{14}O_2$: 361.12341 (M^+ − H); Found 361.12274.

General procedure for preparative photolyses

All preparative photolyses were carried out in a Rayonet photoreactor at 300 and 350 nm (16 lamps). 100 mL of sample solutions ($c \sim 10^{-3}$ M) were prepared in a quartz tube and purged with argon for 20 min prior to and continuously during the

irradiation. Cooling was achieved by a tap water cold finger. After irradiation, 100 mL of water was added and extracted by CH_2Cl_2 (3 × 50 mL). The combined organic layers were dried over anhydrous $MgSO_4$ and the solvent was removed under reduced pressure. If photolyses were carried out in a neat organic solvent, the extraction step was not performed. The residue was then purified if necessary by preparative TLC plates and then characterized by NMR and MS.

Photolysis of 1-(2,5-dihydroxyphenyl)naphthalene (9) in CH_3CN. A solution of 30 mg (0.127 mmol) of **9** in 100 mL of neat CH_3CN was irradiated for 10 h at 300 nm under argon purge. The crude residue was chromatographed on a thin layer of silica using 25% ethyl acetate in hexanes as an eluent to afford the following photoproducts:

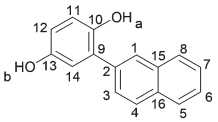

2-(2,5-Dihydroxyphenyl)naphthalene (16).[30b] 18 mg (60%); colorless crystals; mp: 171–173 °C (Lit.[30b] mp = 173 °C); ^{1}H NMR (500 MHz, CD_3CN) δ 7.98 (d, J = 1.5 Hz, 1 H, H-1), 7.90–7.88 (m, 3 H, H-4, H-5 and H-8), 7.66 (dd, J = 8.7, 1.5 Hz, 1 H, H-3), 7.51–7.49 (m, 2 H, H-6 and H-7), 6.83 (d, J = 3.1 Hz, 1 H, H-14), 6.79 (d, J = 8.7 Hz, 1 H, H-11), 6.68 (dd, J = 8.7, 3.1 Hz, 1 H, H-12), 6.55 (s, 1 H, OHb), 6.42 (s, 1 H, OHa); ^{13}C NMR (125 MHz, CD_3CN) δ 150.7 (s, C-13), 147.2 (s, C-10), 136.3 (s, C-2), 133.6 (s, C-15), 132.6 (s, C-16), 129.2 (s, C-9), 128.1 (d, C-8), 127.9 (d, C-3/1) 127.7 (d, C-5/4), 127.6 (d, C-5/4), 126.3 (d, C-6/7), 126.1 (d, C-6/7), 117.2 (d, C-11/14), 117.1 (d, C-11/14), 115.5 (d, C-12).

HMBC interactions: H-1 and C-3, C-9, C-16; H-3 and C-1, C-16; H4/5/8 and C-6/7, C-4/5, C-16, C-15, C-2; H-6 and C-8, C-16; H-7 and C-5, C-15; H-14 and C-1, C-2, C-10; H-11 and C-9, C-10, C-13; H-12 and C-14, C-10; OHb and C-13, C-14; OHa and C-9, C-11, C-10.

NOE interactions: H-1 and H-8; H-1 and H-14; H-3 and H-14.

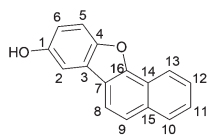

Naphtho[1,2-*b*]benzofuran-8-ol (17).[31] 3 mg (9%); yellow solid; ^{1}H NMR (500 MHz, $CDCl_3$) δ 8.41 (d, J = 8.2 Hz, 1 H, H-13), 7.96 (d, J = 8.2 Hz, 1 H, H-10), 7.91 (d, J = 8.6, 1 H, H-8), 7.73 (d, J = 8.6 Hz, 1 H, H-9), 7.62 (t, J = 7.8 Hz, 1 H, H-12), 7.56–7.53 (m, 2 H, H-5 and H-11), 7.40 (d, J = 2.4 Hz, 1 H, H-2), 6.96 (dd, J = 8.7 Hz, 2.4 Hz, 1 H, H-6), 4.86 (s, 1 H, OH); ^{13}C NMR (125 MHz, $CDCl_3$) δ 153.2 (s, C-16), 151.8 (s, C-1), 151.1 (s, C-4), 133.3 (s, C-15), 128.6 (d, C-10), 126.6 (d, C-12), 126.4 (d, C-11), 126.1 (s, C-3), 124.1 (d, C-9), 123.2 (s, C-14), 121.7 (d, C-13), 121.2 (s, C-7), 119.3 (d, C-8), 118.7 (d, C-8), 114.6 (d, C-6), 112.5 (d, C-5), 106.0 (d, C-2).

HMBC interactions: H-13 and C-11, C-15, C-16; H-10 and C-13, C-9, C-12; H-8 and C-15, C-3, C-9, C-7; H-9 and C-7, C-14, C-10, C-15; H-12 and C-14, C-10; H-11 and C-13, C-15; H-5 and C-3, C-1, C-4; H-2 and C-4, C-6, C-7, C-5; H-6 and C-4, C-2; OH and C-2, C-6, C-1.

NOE interactions: H-13 and H-12; H-5 and H-6; H-10 and H-11; H-8 and H-9; H-2 and H-8.

Photolysis of 9 in 1 : 9 H_2O–CH_3CN. A solution of 30 mg (0.127 mmol) of **9** in 100 mL of 5% H_2O–CH_3CN was irradiated at 300 nm for 1 h under argon purge. The crude residue was analyzed by ^{1}H NMR which showed a mixture of starting material **9** and single photoproduct **19** (~71% conversion). The crude residue was chromatographed on a thin layer of silica using 35% ethyl acetate in hexanes as an eluent to afford photoproduct **19** as a single product.

6,6a-Dihydrobenzo[*kl*]xanthen-10-ol (19). 16 mg (53%); pale yellow oil; ^{1}H NMR (500 MHz, $CDCl_3$) δ 7.48 (d, J = 7.5 Hz, 1 H), 7.33 (t, J = 7.7 Hz, 1 H), 7.22 (d, J = 2.9, 1 H), 7.18 (t, J = 7.7 Hz, 1 H), 6.24–6.18 (m, 2 H), 5.31–5.29 (m, 1 H), 4.56 (s, 1 H, OH), 3.47–3.37 (m, 2 H); ^{13}C NMR (125 MHz, $CDCl_3$) δ 150.6 (s), 149.6 (s), 132.0 (s), 130.3 (s), 128.6 (s), 128.0 (d), 127.4 (d), 127.3 (d), 125.3 (d), 124.8 (s), 120.3 (d), 118.3 (d), 116.3 (d), 109.9 (d), 69.7 (d), 29.6 (t). IR ($CHCl_3$, cm^{-1}) 3651, 3620, 3046, 2360, 1650, 1488, 1203, 745.

Photolysis of 9 in 1 : 9 D_2O–CH_3CN. A solution of 15 mg (0.064 mmol) of **9** in 100 mL of 1 : 9 D_2O–CH_3CN was irradiated at 300 nm for 1 h under argon purge. The crude residue was analyzed by ^{1}H NMR, which showed a mixture of **9**-2′D and **19**-7′D in a 48 : 52 ratio. The area of the peak corresponding to the 2′-position of **9** (δ 7.91) was reduced by 60%, indicating a 40 : 60 ratio of **9** to **9**-2′D present in the sample. Runs at different D_2O concentrations were performed in the same way. Results from these runs are shown in Fig. 3.

Photolysis of 10 in CH_3CN. A solution of 30 mg (0.105 mmol) of **10** in 100 mL of neat CH_3CN was irradiated for 2 h at 300 nm under argon purge. The crude residue was analyzed by ^{1}H NMR which showed a mixture of **10**, **20** (~8% conversion), **21** (<2%) and a trace amount of phenanthrene. Preparative TLC (25% ethyl acetate in hexanes) was used to isolate minor product **21**, whose structure was confirmed by comparison to the ^{1}H NMR of the authentic material reported in the literature.[32]

Photolysis of 10 in CH_3OH. A solution of 30 mg (0.105 mmol) of **10** in 100 mL of neat CH_3OH was irradiated for 3 h at 300 nm under argon purge. The crude residue was chromatographed on a thin layer of silica using 40% ethyl acetate in hexanes as an eluent to afford **24** as a single photoproduct:

2-(10-Methoxy-9,10-dihydro-phenanthren-9-yl)-benzene-1,4-diol (24). 23 mg (68%); light yellow oil; ^{1}H NMR (500 MHz, $CDCl_3$) δ 7.92 (d, J = 7.6 Hz, 1 H), 7.89 (d, J = 7.8 Hz, 1 H), 7.42 (dt, J = 7.6, 1.6, 1 H), 7.39 (dt, J = 7.6, 1.6 Hz, 1 H), 7.30–7.18 (m, 4 H), 6.64 (d, J = 8.5 Hz, 1 H), 6.48 (dd, J = 8.5, 3.1 Hz, 1 H), 5.84 (d, J = 3.1 Hz, 1 H), 4.88 (d, J = 3.3 Hz, 1 H), 4.75 (s, 1 H, OH), 4.50 (d, J = 3.3 Hz, 1 H), 4.12 (s, 1 H, OH), 3.34 (s, 3 H, OMe); ^{13}C NMR (125 MHz, $CDCl_3$) δ 149.5 (s), 147.3 (s), 134.1 (s), 133.1 (s), 130.6 (d), 130.5 (d), 129.4 (d), 128.7 (d), 128.0 (d), 127.6 (d, C-16), 124.2 (d), 123.8 (d), 116.8 (d), 116.4 (d), 114.3 (d), 81.1 (d, C-10), 77.4 (d), 56.8 (q, OMe), 44.1 (d, C-1).

Photolysis of 10 in 1 : 1 H_2O–CH_3CN. A solution of 30 mg (0.105 mmol) of **10** in 100 mL of 1 : 1 H_2O–CH_3CN was irradiated for 2 h at 300 nm under argon purge. The crude residue was analyzed by ^1H NMR which showed a mixture of **10**, **22** (~21% conversion), and a trace amount of **23**. Preparative TLC (35% ethyl acetate in hexanes) was used to isolate **23** as the only photoproduct, whose structure was confirmed by comparison to the ^1H NMR of the authentic material reported in the literature.[32]

Naphtho[1,2,3-*kl*]xanthen-11-ol (23). ^1H NMR (500 MHz, $CDCl_3$) δ 7.49–7.47 (m, 2 H), 7.35–7.33 (m, 2 H), 7.25–7.21 (m, 4 H), 6.67 (d, J = 3.0 Hz, 1 H), 6.49 (dd, J = 8.6, 3.0 Hz, 1 H), 6.45 (d, J = 8.6 Hz, 1 H), 5.86 (s, 1 H), 4.47 (s, 1 H), 4.33 (s, 1 H, OH).

Photolysis of 10 in 1 : 9 D_2O–CH_3CN. A solution of 5 mg of **10** in 50 mL of 1 : 9 D_2O–CH_3CN was prepared and each was irradiated at 300 nm (8 lamps, 16 lamps) for 1 min to 5 min. Deuterium incorporation into the substrate was observed by ^1H NMR on the basis of comparison to the spectrum of an authentic material ^1H NMR spectrum.

Photolysis of 11 in CH_3CN. A solution of 30 mg (0.083 mmol) of **11** in 100 mL of neat CH_3CN was irradiated for 1 h at 350 nm under argon purge. The crude residue was chromatographed on a thin layer of silica using 25% ethyl acetate in hexanes as an eluent to afford **28** as a single product.

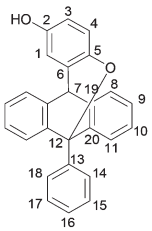

6-Phenyl-6,11-dihydro-6,11-[1,2]benzenodibenzo[*b*,*e*]oxepin-2-ol (28). 28 mg (95%); off-white solid; mp: 168–170 °C; ^1H NMR (500 MHz, $CDCl_3$) δ 8.36 (d, J = 7.7 Hz, 1 H, H-14), 7.64 (t, J = 7.7 Hz, 1 H, H-15), 7.48 (tt, J = 7.4, 1.3, 1 H, H-16), 7.42 (t, J = 7.4 Hz, 1 H, H-17), 7.39 (dd, J = 7.4, 1.0 Hz, 2 H, H-8), 7.22 (td, J = 7.7, 1.3 Hz, 2 H, H-9), 7.10 (td, J = 7.7 Hz, 1.3 Hz, 3 H, H-10, H-18), 6.84 (d, J = 7.7 Hz, 2 H, H-11), 6.71 (d, J = 2.9 Hz, 1 H, H-1), 6.65 (d, J = 8.6 Hz, 1 H, H-4), 6.53 (dd, J = 8.6, 2.9 Hz, 1 H, H-3), 4.61 (s, 1 H, H-7), 4.43 (s, 1 H, OH); ^{13}C NMR (125 MHz, $CDCl_3$) δ 149.0 (s, C-6), 146.6 (s, C-5), 143.4 (s, C-19), 139.4 (s, C-13), 137.8 (s, C-20), 129.8 (d, C-18), 128.4 (d, C-9), 128.3 (d, C-15), 127.8 (d, C-11), 127.6 (d, C-16), 127.4 (d, C-14), 126.9 (d, C-10 and C-17), 124.1 (d, C-8), 120.7 (d, C-4), 115.5 (d, C-3), 113.5 (d, C-1), 81.9 (s, C-12), 52.3 (d, C-7); IR ($CHCl_3$, cm^{-1}) 3381, 3075, 3046, 2360, 1650, 1491, 1437, 1203, 735; MS (ESI) HRMS, calcd for $C_{20}H_{14}O_2$: 361.12341 ($M^+ - H$); Found 361.12264.

HMBC interactions: H-7 and C-5; H-3 and C-1, C-5; H-4 and C-5, C-6; H-1 and C-7, C-3, C-5; H-11 and C-12, C-9; H-10 and C-8, C-20; H-18 and C-16; H-9 and C-19, C-8, C-11; H-8 and C-20, C-10; H-17 and C-13, C-15; H-16 and C-18, C-14; H-15 and C-17, C-13; H-14 and C-18.

NOE interactions: H-7 and H-1; H-7 and H-8; H-3 and H-4; H-10.

Photolyses of 12, 13 and 15 in CH_3CN. All the methyl ether precursors **12**, **13** and **15** were irradiated under similar conditions, no observable photoproducts were formed, suggesting that all the above photoreactions require the phenolic OH to proceed through proton transfer for the indicated reactions.

Quantum yields

Quantum yields of deuterium incorporation (Φ_{ex}) and (Φ_{cyc}) for **9** and **10** were measured by comparison with the deuterium exchange and cyclization of **1** as a secondary actinometer (Φ_{ex} = 0.14; Φ_{cyc} = 0.20). A known amount of **9** and **10** was dissolved in 10% D_2O–CH_3CN (50 mL), neat CH_3CN, or CH_3OH in a quartz tube and irradiated long enough to give a low conversion (5 min for **9**; 1 min for **10**) in a Rayonet reactor at 300 nm (8 or 16 lamps). After irradiation, 50 mL of H_2O was added and extractions with CH_2Cl_2 (3 × 50 mL) were carried out. The extracts were dried over anhydrous $MgSO_4$. In order to obtain more accurate quantum yield for DHPA **10**, another secondary actinometer 2-phenyl-1-naphthol (**31**) (Φ_{ex} = 0.7)[17] was employed. An equimolar amount of **1** or **31** was irradiated under the same conditions. Each run, the system was maintained at ~15 °C by an internal cooling finger and purged with argon for 15 min prior to irradiation. After aqueous workup, extraction and removal of the solvent, extent of the deuterium incorporation or corresponding photochemical reactions were determined by ^1H NMR. Integration from ^1H NMR was used to determine the relative conversion of deuterium exchanges, cyclization or corresponding photochemical reactions. All the values are the results from at least three independent irradiations. Alternatively, quantum yields for photochemical cyclization of **11** were calculated by comparison with the deuterium exchange of 9-(2-hydroxyphenyl)anthracene as a secondary actinometer (Φ_{ex} = 0.09).[16a] Following the same procedures above, the irradiations were operated in a Rayonet reactor at 350 nm (16 lamps).

UV-vis studies

Solutions (10^{-5} M) in the indicated solvent system were prepared in 1.0 cm quartz cuvettes (3.0 mL) and purged with a stream of nitrogen gas by a syringe needle for 5 min prior to measurements. Irradiations were carried out in a Rayonet 100 photoreactor at 300 or 350 nm (16 lamps). The cooling system was achieved by fan. The irradiation was stopped at regular time intervals and each UV-vis trace was recorded.

Steady state and time-resolved fluorescence measurements

Fluorescence spectra were not corrected for spectral response. Since only relative changes were studied based on fluorescence emission from known chromophores, uncorrected spectra sufficed for the mechanistic studies in this work. Steady-state fluorescence measurements were conducted on a Photon Technology International (PTI) Quanta-Master luminescence spectrometer. All the samples dissolved in CH_3CN with OD < 0.1 at the excitation wavelength (310, 320, 330 or 340) were

purged with nitrogen for 15 min prior to analysis. The measurements were performed at 20 °C. Fluorescence quantum yields were determined by comparison of the integration of the emission band with that of quinine bisulfate (Φ_f = 0.55 in 1.0 N H_2SO_4),[23] followed by correction for the differences in the refractive index. Measurements were recorded at three different excitation wavelengths and three quantum yields were calculated and the mean value was reported. Fluorescence lifetimes (τ_f) were measured on an instrument with light emitting diode (excitation wavelength = 310 nm), utilizing a time-correlated single photon counting technique in 1023 channels. Histograms of the instrument response functions using LUDOX scatterer and sample decays were recorded until they typically reached 3×10^3 counts in the peak channel.

Laser flash photolysis (LFP)

All LFP studies were conducted employing a YAG laser, with a pulse width of 10 ns and an excitation wavelength of 266 nm. Static cells (0.7 cm) were used and solutions were purged with N_2 and O_2 for 20 min prior to the measurements. Absorbances at 266 nm were ~0.4.

Acknowledgements

We thank the Natural Sciences and Engineering Research Council (NSERC) of Canada and the University of Victoria for financial support.

Notes and references

1 (*a*) J. F. Ireland and P. A. H. Wyatt, Acid–base properties of electronically excited states of organic molecules, *Adv. Phys. Org. Chem.*, 1976, **12**, 131–221; (*b*) W. Klöpffer, *Adv. Photochem.*, 1977, **10**, 311; (*c*) L. G. Arnaut and S. J. Formosinho, Excited-state proton transfer reactions I. Fundamentals and intermolecular reactions, *J. Photochem. Photobiol., A*, 1993, **75**, 1–20; (*d*) S. J. Formosinho and L. G. Arnaut, Excited-state proton transfer reactions II. Intramolecular reactions, *J. Photochem. Photobiol., A*, 1993, **75**, 21–48; (*e*) S. M. Ormson and R. G. Brown, Excited state intramolecular proton transfer part 1: ESIPT to nitrogen, *Prog. React. Kinet.*, 1994, **19**, 45–91; (*f*) D. Le Gourriérec, S. M. Ormson and R. G. Brown, Excited state intramolecular proton transfer part 2: ESIPT to oxygen, *Prog. React. Kinet.*, 1994, **19**, 211–275; (*g*) N. Agmon, Elementary steps in excited state proton transfer, *J. Phys. Chem. A*, 2005, **109**, 13–35; (*h*) *Hydrogen-transfer Reactions*, ed. J. T. Hynes, J. P. Klinman, H.-H. Limbach and R. L. Schowen, Wiley-VCH, Weinheim, 2007.

2 A. Z. Weller, Innermolekularer protonenübergang im angeregten zustand, *Z. Elektrochem.*, 1956, **60**, 1144–1147.

3 (*a*) M. J. Paterson, M. A. Robb, L. Blancafort and A. D. DeBellis, Mechanism of an exceptional class of photostabilizers: a seam of conical intersection parallel to excited state intramolecular proton transfer (ESIPT) in *o*-hydroxyphenyl-(1,3,5)-triazine, *J. Phys. Chem. A*, 2005, **109**, 7527–7537; (*b*) T. P. Smith, K. A. Zaklika, K. Thakur, G. C. Walker, K. Tominaga and P. F. Barbara, Ultrafast studies on proton transfer in photostabilizers, *J. Photochem. Photobiol., A*, 1992, **65**, 165–175.

4 (*a*) D. Y. Han, J. M. Kim, J. Kim, H. S. Jung, Y. H. Lee, J. F. Zhang and J. S. Kim, ESIPT-based anthraquinonylcalix-[4]crown chemosensor for In^{3+}, *Tetrahedron Lett.*, 2010, **51**, 1947–1951; (*b*) F. F. Oliveira, D. C. Santos, A. A. Lapis, J. R. Correa, A. F. Gomes, F. C. Gozzo, C. Fabio, P. F. Moreira, V. C. de Oliveira, F. H. Quina and B. A. Neto, On the use of 2,1,3-benzothiadiazole derivatives as selective live cell fluorescence imaging probes, *Bioorg. Med. Chem. Lett.*, 2010, **20**, 6001–6007.

5 (*a*) J. M. Kauffman, Review of progress on scintillator fluors for the detectors of the SSC, *Radiat. Phys. Chem.*, 1993, **41**, 365–371; (*b*) A. Pla-Dalmau, 2-(2′-Hydroxyphenyl)benzothiazoles, benzoxazoles, and benzimidazoles for plastic scintillation applications, *J. Org. Chem.*, 1995, **60**, 5468–5473.

6 (*a*) F. Vollmer and W. Rettig, Fluorescence loss mechanism due to large-amplitude motions in derivatives of 2,2′-bipyridyl exhibiting excited-state intramolecular proton transfer and perspectives of luminescence solar concentrators, *J. Photochem. Photobiol., A*, 1996, **95**, 143–155; (*b*) D.-Y. Chen, C.-L. Chen, Y.-M. Cheng, C.-H. Lai, J.-Y. Yu, B.-S. Chen, C.-C. Hsieh, H.-C. Chen, L.-Y. Chen, C.-Y. Wei, C.-C. Wu and P.-T. Chou, Design and synthesis of trithiophene-bound excited-state intramolecular proton transfer dye: enhancement on the performance of bulk heterojunction solar cells, *ACS Appl. Mater. Interfaces*, 2010, **2**, 1621–1629.

7 (*a*) K. Sakai, M. Takemura and Y. Kawabe, Lead chloride-based layered perovskite incorporated with an excited state intramolecular proton transfer dye, *J. Lumin.*, 2010, **130**, 2505–2507; (*b*) M. Kasha, Proton-transfer spectroscopy and proton-transfer lasers, *Acta Phys. Pol., A*, 1987, **71**, 717–729; (*c*) S. Park, O.-H. Kwon, S. Kim, S. Park, M.-G. Choi, M. Cha, S. Y. Park and D.-J. Jang, Imidazole-based excited-state intramolecular proton-transfer materials: synthesis and amplified spontaneous emission from a large single crystal, *J. Am. Chem. Soc.*, 2005, **127**, 10070–10074; (*d*) D. A. Parthenopoulos, D. P. McMorrow and M. Kasha, Comparative study of stimulated proton transfer luminescence of three chromones, *J. Phys. Chem.*, 1991, **95**, 2668–2674; (*e*) A. Douhal, F. Amat-Guerri, A. U. Acuňa and K. Yoshihara, Picosecond vibrational relaxation in the excited-state proton-transfer of 2-(3′-hydroxy-2′-naphthyl) benz-imidazole, *Chem. Phys. Lett.*, 1994, **217**, 619–625.

8 B. Valeur, *Molecular Fluorescence: Principles and Applications*, Wiley-VCH Verlag GmbH, Weinheim, 2001, ch. 4, pp. 99–106.

9 M. Kasha, Proton-transfer spectroscopy: perturbation of the tautomeriztion potential, *J. Chem. Soc., Faraday Trans. 2*, 1986, **82**, 2379–2392.

10 J. Wirz, Kinetics of proton transfer reactions involving carbon, *Pure Appl. Chem.*, 1998, **70**, 2221–2232.

11 (*a*) N. A. O'Connor, A. J. Berro, J. R. Lancaster, X. Gu, S. Jockusch, T. Nagai, T. Ogata, S. Lee, P. Zimmerman, C. G. Willson and N. J. Turro, Toward the design of a sequential two photon photoacid generator for double exposure photolithography, *Chem. Mater.*, 2008, **20**, 7374–7376; (*b*) R. M. D. Nunes, M. Pineiro and L. G. Arnaut, Photoacid for extremely long-lived and reversible pH-jumps, *J. Am. Chem. Soc.*, 2009, **131**, 9456–9462; (*c*) J. E. Kwon and S. Y. Park, Advanced organic optoelectronic materials: harnessing excited-state intramolecular proton transfer (ESIPT) process, *Adv. Mater.*, 2011, **23**, 3615–3642.

12 (*a*) H. Shizuka, Excited state proton-transfer reaction and proton-induced quenching of aromatic compounds, *Acc. Chem. Res.*, 1985, **18**, 141–147; (*b*) L. M. Tolbert and K. M. Solntsev, Excited-state proton transfer: from constrained systems to "super" photoacids to superfast proton transfer, *Acc. Chem. Res.*, 2002, **35**, 19–27; (*c*) T. Förster, *Pure Appl. Chem.*, 1970, **24**, 443; (*d*) P. Wan and D. Shukla, *Chem. Rev.*, 1993, **93**, 571–584; (*e*) M. Lukeman and P. Wan, in *Handbook of organic photochemistry and photobiology*, ed. W. Horspool and F. Lenci, CRC Press, Boca Raton, FL, 2nd edn, 2004, ch. 39, pp. 1–19; (*f*) P. Wan, B. Barker, L. Diao, M. Fischer, Y. Shi and C. Yang, 1995 Merck Frosst Award Lecture. Quinone methides: relevant intermediates in organic chemistry, *Can. J. Chem.*, 1996, **74**, 465–475.

13 (*a*) P. Wan, D. W. Brousmiche, C. Z. Chen, J. Cole, M. Lukeman and M. Xu, Quinone methide intermediates in organic photochemistry, *Pure Appl. Chem.*, 2001, **73**, 529–534; (*b*) M. Lukeman and P. Wan, Excited state intramolecular proton transfer (ESIPT) in 2-phenylphenol: an example of proton transfer to a carbon of an aromatic ring, *Chem. Commun.*, 2001, 1004–1005; (*c*) M. Lukeman and P. Wan, A new type of excited-state intramolecular proton transfer: proton transfer from phenol OH to a carbon atom of an aromatic ring observed for 2-phenylphenol, *J. Am. Chem. Soc.*, 2002, **124**, 9458–9464; (*d*) N. Basarić and P. Wan, Excited state proton transfer (ESPT) from phenol to nitrogen and carbon in (2-hydroxyphenyl)pyridines, *Photochem. Photobiol. Sci.*, 2006, **5**, 656–664.

14 M. Lukeman and P. Wan, Excited-state intramolecular proton transfer in *o*-hydroxybiaryls: a new route to dihydroaromatic compounds, *J. Am. Chem. Soc.*, 2003, **125**, 1164–1165.

15 M. Flegel, M. Lukeman and P. Wan, Photochemistry of 1,1′-bi-2-naphthol (BINOL)-ESIPT is responsible for photoracemization and photocyclization, *Can. J. Chem.*, 2008, **86**, 161–169.

16 (*a*) M. Flegel, M. Lukeman, L. Huck and P. Wan, Photoaddition of water and alcohols to the anthracene moiety of 9-(2′-hydroxyphenyl) anthracene *via* formal excited state intramolecular proton transfer, *J. Am. Chem. Soc.*, 2004, **126**, 7890–7897; (*b*) N. Basarić and P. Wan, Competing excited state intramolecular proton transfer pathways from phenol to anthracene moieties, *J. Org. Chem.*, 2006, **71**, 2677–2686; (*c*) Y. Shi and P. Wan, Solvolysis and ring closure of quinone methides photogenerated from biaryl systems, *Can. J. Chem.*, 2005, **83**, 1306–1323.

17 N. Basarić, N. Došlić, J. Ivković, Y.-H. Wang, M. Mališ and P. Wan, Very efficient generation of quinone methides through excited state intramolecular proton transfer to a carbon atom, *Chem.–Eur. J.*, 2012, **18**, 10617–10623.

18 Y.-H. Wang and P. Wan, Excited state intramolecular proton transfer (ESIPT) in dihydroxyphenyl anthracenes, *Photochem. Photobiol. Sci.*, 2011, **10**, 1934–1944.

19 M. Lukeman, *Excited state intramolecular proton transfer (ESIPT) to aromatic carbon*, PhD Dissertation, University of Victoria, Victoria B.C., Canada.

20 (*a*) I. A. Z. Al-ansari, Intramolecular charge transfer states in a series of (2,5-dimethoxyphenyl)-arenes, *J. Photochem. Photobiol., A*, 1993, **72**, 15–21; (*b*) J. Yin, M. P. Rainka, X.-X. Zhang and S. L. Buchwald, A highly active Suzuki catalyst for the synthesis of sterically hindered biaryls: novel ligand coordination, *J. Am. Chem. Soc.*, 2002, **124**, 1162–1163.

21 (*a*) R. Krishnan, T. G. Fillingim, J. Lee and G. W. Robinson, Solvent structural effects on proton dissociation, *J. Am. Chem. Soc.*, 1990, **112**, 1353–1357; (*b*) G. W. Robinson, Proton charge transfer involving the water solvent, *J. Phys. Chem.*, 1991, **95**, 10386–10391; (*c*) N. Agmon, D. Huppert, A. Masad and E. Pines, Excited-state proton transfer to methanol–water mixtures, *J. Phys. Chem.*, 1991, **95**, 10407–10413; (*d*) K. M. Solntsev, D. Huppert, N. Agmon and L. M. Tolbert, Photochemistry of "super" photoacids. 2. Excited-state proton transfer in methanol/water mixtures, *J. Phys. Chem. A*, 2000, **104**, 4658–4669.

22 (*a*) K. M. Solntsev, D. Huppert, L. M. Tolbert and N. Agmon, Solvatochromic shifts of "Super" photoacids, *J. Am. Chem. Soc.*, 1998, **120**, 7981–7982; (*b*) M. Fischer and P. Wan, Nonlinear solvent water effects in the excited-state (formal) intramolecular proton transfer (ESIPT) in *m*-hydroxy-1,1-diaryl alkenes: efficient formation of *m*-quinone methides, *J. Am. Chem. Soc.*, 1999, **121**, 4555–4562.

23 I. B. Berlman, in *Handbook of fluorescence spectra of aromatic molecules*, Academic Press, New York, 1971, p. 363.

24 N. Basarić, N. Došlić, J. Ivković, Y.-H. Wang, J. Veljković, K. Mlinarić-Majerski and P. Wan, Excited state intramolecular proton transfer (ESIPT) from phenol to carbon in selected phenylnaphthols and naphthylphenols, *J. Org. Chem.*, 2013, **78**, 1811–1823.

25 (*a*) L. M. Tolbert and J. Haubrich, Photoexcited proton transfer from enhanced photoacids, *J. Am. Chem. Soc.*, 1994, **116**, 10593–10600; (*b*) M. Fischer and P. Wan, *m*-Quinone methides from *m*-hydroxy-1,1-diaryl alkenes *via* excited-state (formal) intramolecular proton transfer mediated by a water trimer, *J. Am. Chem. Soc.*, 1998, **120**, 2680–2681.

26 (*a*) D. Brousmiche, M. Xu, M. Lukeman and P. Wan, Photohydration and photosolvolysis of biphenyl alkenes and alcohols *via* biphenyl quinone methide-type intermediates and diarylmethyl carbocations, *J. Am. Chem. Soc.*, 2003,

125, 12961–12970; (*b*) Y. Shi and P. Wan, Charge polarization in photoexcited alkoxy-substituted biphenyls: formation of biphenyl quinone methides, *J. Chem. Soc., Chem. Commun.*, 1995, 1217–1218; (*c*) N. Basarić, I. Žabčić, K. Mlinarić-Majerski and P. Wan, Photochemical formation and chemistry of long-lived adamantylidene-quinone methides and 2-adamantyl cations, *J. Org. Chem.*, 2010, **75**, 102–116.

27 N. Basarić, N. Cindro, D. Bobinac, L. Uzelac, K. Mlinarić-Majerski and P. Wan, Zwitterionic biphenyl quinone methides in photodehydration reactions of 3-hydroxybiphenyl derivatives: laser flash photolysis and antiproliferation study, *Photochem. Photobiol. Sci.*, 2012, **11**, 381–396.

28 (*a*) R. A. McClelland, C. Chan, F. L. Cozens, A. Modro and S. Steenken, Laser flash photolysis generation, spectra, and lifetimes of phenylcarbenium ions in trifluoroethanol and hexafluoroisopropyl alcohol. On the UV spectrum of the benzyl cation, *Angew. Chem., Int. Ed. Engl.*, 1991, **30**, 1337–1339; (*b*) F. L. Cozens, V. M. Kanagasabapathy, R. A. McClelland and S. Steenken, Lifetimes and UV-visible absorption spectra of benzyl, phenethyl, and cumyl carbocations and corresponding vinyl cations. A laser flash photolysis study, *Can. J. Chem.*, 1999, **77**, 2069–2082; (*c*) R. A. McClelland, N. Banait and S. Steenken, Electrophilic reactions of xanthylium carbocations produced by flash photolysis of 9-xanthenols, *J. Am. Chem. Soc.*, 1989, **111**, 2929–2935.

29 (*a*) G. Hoffmann, A. Schoenbucher and H. Steidl, Fluorescence yields of triphenylcarbonium derivatives, *Z. Naturforsch., A*, 1973, **28**, 1136–1139; (*b*) A. Azarani, A. B. Berinstain, L. J. Johnston and S. Kazanis, Electron transfer reactions between excited diarylmethyl and triarylmethyl carbocations and aromatic donors, *J. Photochem. Photobiol., A*, 1991, **57**, 175–189; (*c*) M. H. Acar, Y. Yagci and W. Schnabel, Formation of triphenylmethyl cation during the photolysis of phenylazotriphenyl methane: a laser flash photolysis study, *Polym. Int.*, 1998, **46**, 331–335.

30 (*a*) H. Kawafuchi and T. Inokuchi, Novel access to cyclohexane-1,4-diones and 1,4-hydroquinones *via* radical 1,2-acyl rearrangement on 2-(halomethyl)cyclopentane-1,3-diones using cobaloxime-mediated electroreduction or tributyltin hydride, *Tetrahedron Lett.*, 2002, **43**, 2051–2054; (*b*) M.-E. Million, P. Mailliett, H. Chen, G. Bashiardes, J. Boiziau, F. Parker, A. Commercon, B. Tocque, B. P. Roques and C. Garbat, Synthesis and biological evaluation of a new series of phenylhydroquinone derivatives as inhibitors of EGF-R-associated PTK activity, *Anti-Cancer Drug Des.*, 1996, **11**, 129–153.

31 K. Schimmelschmidt, Synthesen in der Diphenylenoxyd-Reihe, *Justus Liebigs Ann. Chem.*, 1950, **566**, 184–206.

32 B. J. Morrison and O. C. Musgrave, Thiones as reactive intermediates in condensations of diketones with aromatics mediated by tetraphosphorus decasulfide, *Phosphorus, Sulfur Silicon Relat. Elem.*, 2002, **177**, 2725–2744.

